ISSN : 0974 - 7494 Volume 8 Issue 6

Nano Science and Nano Technology

An Indian Journal

Review

NSNTAIJ, 8(6), 2014 [227-263]

Non-carbonaceous nanostructured support materials for low temperature fuel cell electrocatalysts

Maryam Yaldagard[1,3]*, Naser Seghatoleslami[1,3], Mohsen Jahanshahi[2,3]

[1]Department of Chemical Engineering, Engineering Faculty, Ferdowsi University of Mashhad, (IRAN)
[2]Department of Chemical Engineering, Engineering Faculty, Noshirvani University of Technology, Babol, (IRAN)
[3]Nanotechnology Research Institute, Noshirvani University of Technology, Babol, (IRAN)
E-mail : m_yaldagard@yahoo.com; ma_ya371@stu-um.ac.ir

ABSTRACT

Highly dispersed platinum or platinum-based catalysts on a conductive support are commonly used as electrode materials in low-temperature fuel cells, particularly the hydrogen PEMFC and the direct methanol PEMFC. The performance and durability/stability of these catalysts strongly depend on the characteristics of the support. Catalysts supported on high surface area carbon black are widely used in low temperature fuel cells. However, the corrosion of carbon black has been recognized as one of major causes of performance degradation and durability issues of low-temperature fuel cells under high-potential conditions. So the need for alternative supports with outstanding physical and mechanical properties to carry out the successful reaction in catalyst layer and give a longer lifetime for the electrocatalysts is inevitable. The emergence of nanothechnology and development of nanostructure materials in recent years has opened up new avenues of materials development for low-temperature fuel cells. This paper presents the performance with a variety of non-carbonaceous nanostructured based materials, e.g metal oxides and carbides nanowires (NWs), nanorods, the nanostructer of conductive polymers e.g. PAni / PPy nanofibers, and PAni / PPy nanowires as well as composites of these nanostructured catalyst support materials. So the present paper provides an overview of these nanostructured materials as low-temperature fuel cell catalyst supports. The improved characteristics of the nanostructured supports with respect to commercially used carbon black (Vulcan XC-72) and their effect on the electrochemical activity are highlighted. Additionally it reviews the literature on the synthesis of nanostructured-supported Pt electrocatalysts for proton exchange membrane (PEM) fuel cell catalyst loading reducing through the improvement of catalyst utilization and activity. The features of each synthetic method were also discussed based on the morphology of the synthesized catalysts.

KEYWORDS

Low temperature fuel cell;
PEMFC;
DMFC;
Pt-based electrocatalyst;
Nanostructured-supports;
Durability/Stability.

INTRODUCTION

In recent years, the concept of green energy has attracted considerable attention. The aim of green energy is to explore techniques and methodologies that reduce or eliminate the generation of products or byproducts that are hazardous to human health or the environment. Nowadays, green energy is becoming one of the main goals of designing new processes and reactions in the emerging areas of nanoscience and nanotechnology[1,2]. Fuel cells are electrochemical conversion devices used for power generation in portable, stationary/residential and transportation applications. As a "green/clean" electric power source, fuel cells can be used to power vehicles, back-up the power supply for electric devices, and store electricity in power stations by converting water into hydrogen and oxygen during off-peak hours. The only by-products are water and heat. Among various types of fuel cells proton exchange membrane fuel cells (also called polymer electrolyte membrane fuel cell, PEMFCs) have been considered to be a promising energy source because they offer a highly efficient, low operation temperature (below 100 °C), higher power density, rapid start up/shut down, low weight, compactness, potential for low cost and volume, long stack life, suitability for discontinuous operation and environment friendly technology for energy conversion without the carnot limitations of combustion engines[3-7]. However, while great progress has been made in the last several decades in the research and development of PEM fuel cells[8-10]. For wide-scale commercialization of PEMFCs it should overcome several technical challenges including reducing the cost of component, optimizing the utilization of electrocatalyst at all current densities, improving the performance and durability/stability of the membrane electrode assembly (MEA), the crucial part of the fuel cell system. As the key component in PEMFC, the electrocatalyst layer is the place where the electrochemical reactions take place and the electrical energy is produced, exhibiting a great influence on the total performance and durability. The main processes that occur in the catalyst layer include mass transport, interfacial reactions at electrochemically active sites, proton transport in the electrolyte phase, and electron conduction in the electronic phase. The PEM fuel cell MEA utilizes precious metal catalyst (such as Pt or Pt alloy) dispersed on support. These catalysts are estimated to contribute to as much as 50% of total fuel cell cost. It was emphasized that in order to reach the DOE (department of energy) cost reduction objects, among other component cost reductions, the current state of the art platinum loading (~0.4 mg/cm^2) of PEM fuel cell electrodes, the total Pt catalyst loading in a MEA must be reduced to levels lower than 0.1 mg/cm^2 to come across the target for commercialization[11]. Similarly, durability targets for these applications have not been mentioned for catalysts, but MEAs are expected to endure for >40,000 and 3,000 hours for stationary and portable applications respectively, with low degradation rates.

Several strategies have been explored with the purpose of reducing the cost and increase the performance of a fuel cell. These active approaches toward the reduction of Pt usage in PEMFC catalyst can generally be listed as:

(i) Reducing Pt usage by alloy with other transition metals (either as bimetallic or ternary catalyst systems) and non-noble electrocatalysts[12-19].
(ii) Reducing the Pt loading in fuel cell electrodes by using ultra-low loading catalyst methods[20-25]
(iii) Thinning the active layer thickness (≤25 micrometer)[26-33]
(iv) Reduction the electrocatalyst nanoparticle size and improvement of PPEMFC performance by optimization of operating parameters[34].
(v) Improving electrocatalyst dispersion by using novel fabrication techniques (e.g. The National Research Council of Canada's Institute for Fuel Cell Innovation (NRC-IFCI), Reactive spray deposition technology (RSDT))[35-42].
(vi) Developing MEA fabrication methods to enable better catalyst dispersion and utilization[43-52]
(vii) Developing novel nano-structured thin-film Pt (e.g. 3M's Nonconductive Whiskers or NSTF - based electrode)[53].
(viii) Improving the performance of carbon-based electrocatalyst support and exploring novel non-carbonaceous electrocatalyst support materials by employing the concept of nanotechnology for increasing the surface area and other properties[54-61]

It is very difficult to keep or improve catalyst layer performance when the catalyst loading is reduced. In order to attain that, great effort must be put on Pt utilization and the enhancement of catalyst activity. Different two routes have been explored for enhancing the utilization of platinum catalyst in PEMFCs, either by reduction the particle size of catalyst or by uniform distribution on the surface of support materials.

The prominence of the support materials in fuel cell catalysis is well documented. Typically, the support provides a physical surface for dispersion of small metal particles, which is necessary for accomplishing high surface area. Carbon is commonly used for supporting nanosized electrocatalyst particles in low temperature fuel cells because of its large specific surface area, high electrical conductivity, and pore structures[62,63]. In spite of the high surface area of the carbon black particle it has two main problems. Carbon black persuades significant mass transfer limitations due to its dense structure (the pore size and pore distribution of carbon black affects the interaction between Nafion ionomer and the catalyst nanoparticles), resulting failure of launching three-phase boundaries among gas, electrolyte and electrocatalyst which lead to a very low Pt utilization. Additionally carbon black is known to endure sever electrochemical oxidation, forming surface oxides which reacting finally to CO_2 ($C+2H_2O \rightarrow CO_2+ 4H^+ + 4e^-$) at the cathode of the fuel cell. The formation of CO2 or corrosion can be accelerated at lower pH and higher potential, humidity and temperature so the life time of potential electrocatalyst can be reduced by poisoning and sintering. The standard potential for the electrochemical oxidation of carbon to carbon dioxide is 0.207 V vs. RHE at 25 °C[64]. During the start up/shut down cycle, the cathode potential of vehicle's fuel cell because of slow oxygen reduction reaction (ORR) may increase to 1.2 - 1.5 V or even higher, therefore, under such PEMFC cathode operation conditions, carbon corrosion is not only thermodynamically viable due to the high potentials (>1.2 V) and high O2 concentrations, but also kinetically enhanced by the elevated temperatures (50–90 °C). As carbon black (Vulcan XC-72) corrodes, noble metal nanoparticles (e.g., Pt) on carbon black will isolate from the electrode and possibly combine to larger particles, resulting in Pt surface area loss, which subsequently lowers the durability of PEM fuel cells[65-67]. Accordingly, corrosion of the support may affect the performance of the PEMFC. Therefore prompted by the thermodynamic instability of carbon, tremendous efforts have been made to identify and develop alternative support materials that show good stability up to voltages of 1.4–1.6 V and improve durability and performance.

Nanostructure materials have attracted great interest in recent years because of their exceptional characterization such as high catalytic activity, mechanical and electrical properties, all of which are obtained by obstructing their dimensions. It is well known that the physical, electrochemical, and electronic properties of nanostructured materials are not the same those of bulk materials. In terms of nanotechnology methodologies towards improving clean energy solution, numerous innovative nanomaterials as a catalyst supports for PEMFCs have been actively investigated. In this context the role of the nanostructure in carbon supports like carbon nanotubes (CNTs), carbon nanofibers (CNFs), carbon arogels, nanoplates of graphene was much highlighted which well reviewed by our another paper(under publication).The higher catalytic activity of Pt and Pt-based catalysts supported on CNTs and CNFs than that of the same catalysts supported on carbon blacks was ascribed to their unique structure and properties such as high surface area, good electronic conductivity and chemical stability[68-72]. Tests carried out in PEM fuel cell conditions indicated that these materials can be more durable and can outlast the lifetime of most widely used Vulcan XC-72[73-75]. More recently, a wide range of nanostructure of ceramic materials and conducting polymers (CPs), such as oxides and carbides nanowires (NWs), nanorods, PAni nanofibers, and PPy nanowires and etc, has been investigated as alternatives to carbon. The main purposes for using nanostructure-supported Pt catalysts are to reduce Pt loading through increasing the catalyst utilization, and improving the catalyst activity and total performance.

Ceramic materials such as conducting oxides are emergent candidates as oxidation resistant catalyst supports. These materials are thermally and electrochemically stable in fuel cell environment and present admirable resistance to corrosion in various electrolytic media. In addition to their high stability in the fuel cell environment, unlike carbon, which does not increase electrocatalytic activities, but runs only as a mechanical support, many metal oxide materials can act as co-catalysts. In reality, it is well known that metal oxides such as TiO_2, SnO_2 and WO_3 enhance the catalytic activity of platinum for fuel oxidation[76-81].

Given their conductive and firm three dimensional structure, conducting polymers can act as suitable supports for polymer electrolyte fuel cell catalysts. CPs with porous structures and high surface areas are employed as a medium to integrate noble metal catalysts for some electrochemical reactions of prominence for application in fuel cells such as hydrogen and methanol oxidation and oxygen reduction[82]. The principal purpose for integrating metallic particles into porous polymeric mediums is to increase the specific area of the active surface and thereby improve catalytic efficiency[83,84]. Moreover, CPs are not only electron conducting, but also proton conducting materials, therefore they can substitute Nafion in the catalyst layer of fuel cell electrode and supply improved performance. In this situation, supposedly only a two-phase boundary is required for electron and ion transfer during reactions in fuel cells compared to the three-phase boundary indispensable when carbon is used as support[85].

Being the use of carbon nanostructured materials, ceramic or polymer nanostructured materials not entirely satisfactory, in the last years hybrid polymer–carbonasous nanostructured materials and ceramic–carbonasous nanostructured materials have been proposed as fuel cell catalyst supports. These hybrid nanostructured materials, possessing the properties of each component, or even with a synergistic effect, would present improved characteristics with respect to the individual nanostructured components.

Although there have been many reviews dealing with the synthesis of noncarbon-based material[85-87] and their characteristics as a novel catalyst support in catalyst preparation, a comprehensive review of the literature on the noncarbon-based material nanostructured support which have emphasized the PEM fuel cell application based of our knowledge has not been tried.

This review will focus on some recent developments and investigations of noncarbon-based nanostructure materials and composite of these nanostructured materials with carbon-based nanomaterials for application as support for preparation of electrocatalyst for MEAs purpose, excluding electrolyte membrane and other parts of fuel cell. The structure, dispersity and morphology of the supported catalysts, which are closely related to utilization and performance, are strongly influenced both by the support property and the method by which Pt nanoparticles can be deposited into the support. In this study, the development of low-temperature fuel cell catalysts in recent years is reviewed, primarily focusing on the two most active areas, i.e. support materials especially supports with tailored nanostructural, surface chemical and electronic properties by employing the concept of nanotechnology and nanoscience in designs and production techniques and Pt-based material deposition approaches.

Considering the recent move of a large variety of the public converging to NWs and CPs related synthesis techniques, we have restricted broadly to mentioning the title of production methods of these material in the present study rather than a focused opus, which would have been another useful option if one considers numerous research articles about synthesis and processing techniques of the nanostructure of these materials that have been published in this 10 years span. So where necessary, the reader will be addressed to more specific recent review papers and books. After some simple background information the structure of each of these materials, the basic deposition techniques of Pt-based metals onto the support materials along with the surface functionalization of these nanostructures, characterization and other features of resulted supported electrocatalyst such as morphology, electrochemical activity as well as electrochemical surface area will be described. Next, it will be continued by describing fabrication processes of MEA fuel cells containing nanostructures. This is will be followed by investigation the improvement of utilization of elctrocatalyst and performance in single cell measurements. Finally, we give a summary of the stability/durability of the nanostructure-based fuel cell electrodes. Our focus will be on low-temperature fuel cells including only hydrogen and methanol fuelled polymer electrolyte membrane fuel cells (H-PEMFCs [hydrogen fuel cell] and DMFCs [direct methanol fuel cells]). The direct ethanol fuel cell (DEFC) is also sometimes comprised in low-temperature fuel cells. The term ‘PEMFC’ has been used often to cover the circumstances where DMFC is also applicable unless otherwise specifically mentioned separately.

Inorganic oxide/ carbid nanostructure-supported pt-based electrocatalysts: synthesis, characterization and performance of pem fuel cell

Inorganic metal oxides have been studied to determine whether they can serve as high corrosion resistant supports. Regrettably, substituting carbon with traditional metal-oxides is problematic, due to their electrical-insulating natures at temperatures below 200 °C. However, substoichiometric metal oxides, such as reduced oxidation state titania (e.g., Ti_4O_7 and Ebonex), doped metal oxides(e.g. doped TiO_2 and SnO_2) and nanostructured metal oxides, such as TiO_2 nanotubes and WO_3 nanorods, have been proposed as electrically conductive support materials with high corrosion-resistant properties. Recently Antolini and Gonzalez[105] and Sharma and Pollet[106] have published a detailed reviews on the use of ceramic based materials and Non-Carbonaceous (inorganic oxide/ carbid) support respectively in various aspect of fuel cells and the readers are invited to referred to them. but in this section because of the aim of present study on the use of nanostructure of formentioned materials as support for fuel cell application we only focuses on these materials namely just nanowires, nanorod and nanotube structure of these materials.

Nanoscale one-dimensional (1D) materials have inspired great interest due to their importance in basic scientific research and potential technology applications[88-90]. Nanowires, nanobelts, nanorods, etc are a novel quasi-one dimensional materials that have been attracting a great research interest in the last few years. These non-carbonaceous materials have been established to show superior electrical, optical, mechanical and thermal properties, and can be used as fundamental building blocks for nano-scale science and technology, ranging from chemical and biological sensors, field effect transistors to fuel cell applications. Nature magazine recently published a report titling that “Nanowires, nanorods, nanowhiskers, it does not matter what you call them, they are the hottest property in nanotechnology” (Nature 419 (2002) 553). As an example, Figure 1 shows a collection of various nanostructures of ZnO synthesized by thermal evaporation of solid powders[91].

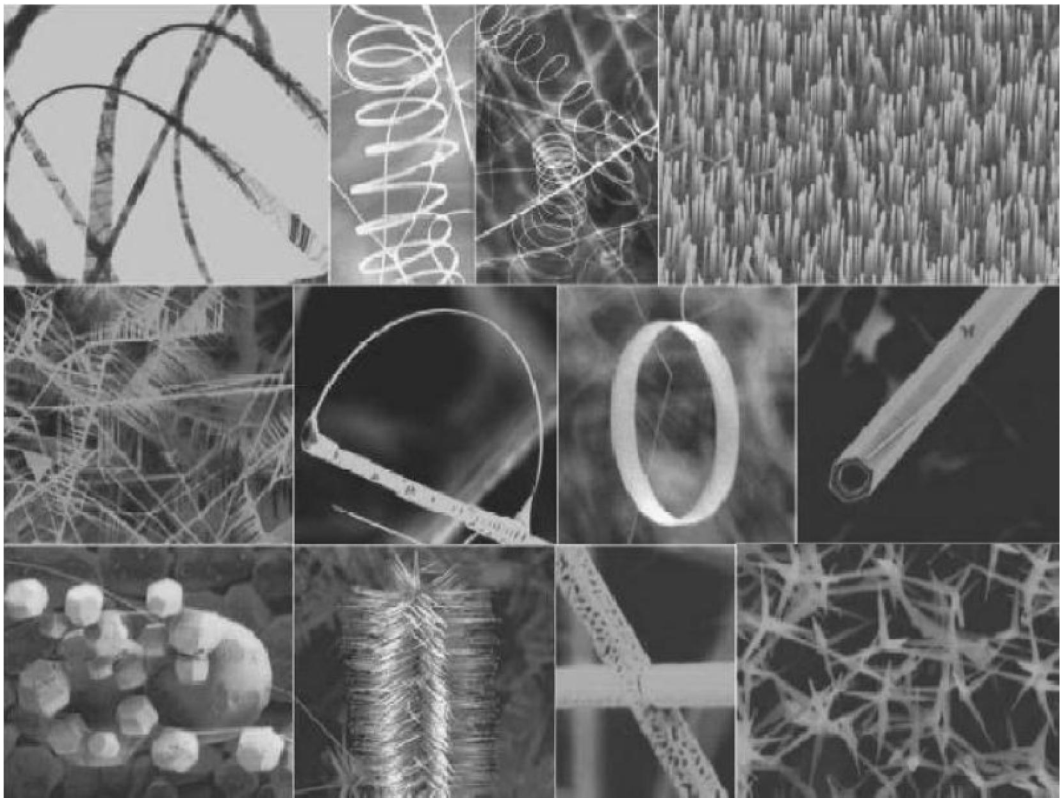

Figure 1 : A collection of nanostructures of ZnO synthesized under controlled conditions by thermal evaporation of solid powders[91]

Nanowires

Structure and synthesis methods for nanowires

Nanowires (NWs), like CNTs, are also one-dimensional and well-defined crystalline structure with a high aspect ratio. NWs have demonstrated superior electrical, optical, mechanical and thermal properties[92-95]. Unlike CNTs, NWs are noncarbon based materials that can consist of metals, semiconductors, or inorganic compounds. The unique feature of nanowires, compared to other low dimensional systems, is that they have two quantum confined directions while still leaving one unconfined direction for electrical conduction. This allows nanowires to be used in applications where electrical conduction rather than tunneling transport is required. Because of the unique density of electronic states nanowires in the limit of small diameters are expected to exhibit significantly different optical, electrical and magnetic properties from their bulk 3D crystalline corresponding item[96]. The broad choice of various crystalline materials and doping methods make the electronic and optical properties of NWs adaptable with a high degree of freedom and precision. With the development of new synthesis methods, NWs have attracted more and more attention for fuel cell applications. There are a few papers[95,97] and books[98-101] dealing with the synthesis, characterization, properties and applications of NWs. A great challenge is to integrate NWs into multi-function assemblies in order to fabricate nanoscale electronic and photonic devices as well as biosensors.

Previously, nanowires with different compositions have been explored, using various methods including vapor phase transport process[102-104], chemical vapor deposition[105,106], arc-discharge[107] solution[108,109] and template-based method[110,111] Recently, a variety of 1D nanostructures with different compositions such as ZnO, SnO_2, WO_3, In_2O_3, CdO, MgO_2, MnO_2, TiO_2 and PbO_2 were successfully synthesized[112-114]. Unlike CNTs, nanowires (NWs) can be made of various compositions of materials with solid cores. For example, monometallic Pt, Au and Ag nanowires[115-117] and Pt nanowire networks[118] synthesized in highly ordered SBA-15 silica have been reported.

NW-supported pt-based electrocatalysts, MEA fabrication and performance of PEM fuel cell

Using NWs, especially metal and metal oxide NWs, as supports for Pt nanoparticles have unique advantages for real applications. First, unlike carbon black, metal oxide materials have catalytic properties. Second, there is a very strong interaction between Pt nanoparticles and the metal oxide surface. Third, gas permeability is expected to be high with the 3D electrode structure with nanowires that are grown on fuel cell backings like carbon paper. Finally, doping various elements into nanowires can be easily carried out to improve electronic conductivity, corrosion resistance, and thermal stability. Therefore, it is expected that integrated three-dimensional, nanowire-based, fuel cell electrodes will be ideal materials for providing a higher catalytic performance, higher catalyst utilization, a more efficient mass transport, and a longer fuel cell operational life. More recently, various metal oxides have been explored as catalyst support[119-122]. Among of them, SnO_2 particles as Pt support have been used for PEMFCs and DMFCs and have revealed high catalytic activities toward methanol oxidation[123,124] and their combination with Pt metal catalyst significantly enhanced the overall catalytic activities. Moreover, there is a strong metal-support interaction between Pt nanoparticles and metal oxide surface[125]

While all of these studies utilized its form of the particles, Saha and coworkers[126] interests, for the first time, was to directly grow SnO_2 nanowires (NWs) on fuel cell backings as catalyst support for fuel cells in order to build 3-D electrode structure. They successfully deposited Platinum–ruthenium (Pt–Ru)

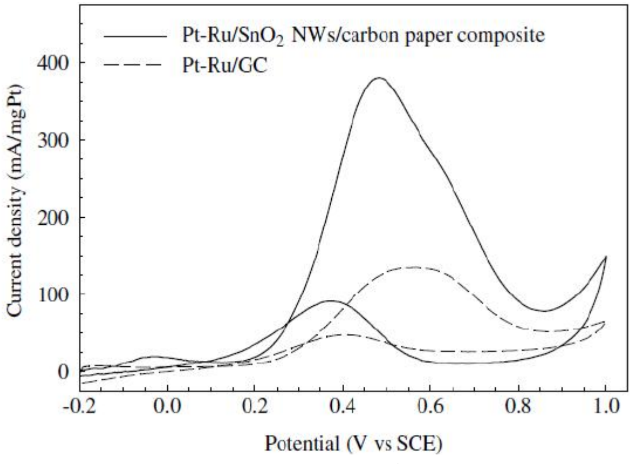

Figure 2 : Cyclic voltammograms of Pt–Ru nanoparticles electrodeposited on SnO2 NWs/carbon paper and GC electrodes in Ar-saturated 1M H2SO4 + 2M MeOH aqueous solution. Potential scan rate: 50 mV/s[126]

nanoparticles on the surface of SnO_2 nanowires grown directly on carbon paper (Pt–Ru/SnO_2 NWs/carbon paper) by potentiostatic electrodeposition method. According to their paper the electrocatalytic activities of these composite electrodes for methanol oxidation were investigated and higher mass and specific activities in methanol oxidation were exhibited as compared to Pt–Ru catalysts deposited on glassy carbon electrode. Figure 2 shows a comparison of catalytic activities for Pt–Ru nanoparticles supported SnO_2 NWs/carbon paper and GC electrodes in 2 M CH_3OH/1 M H_2SO_4 at a scan rate of 50 mV/s.

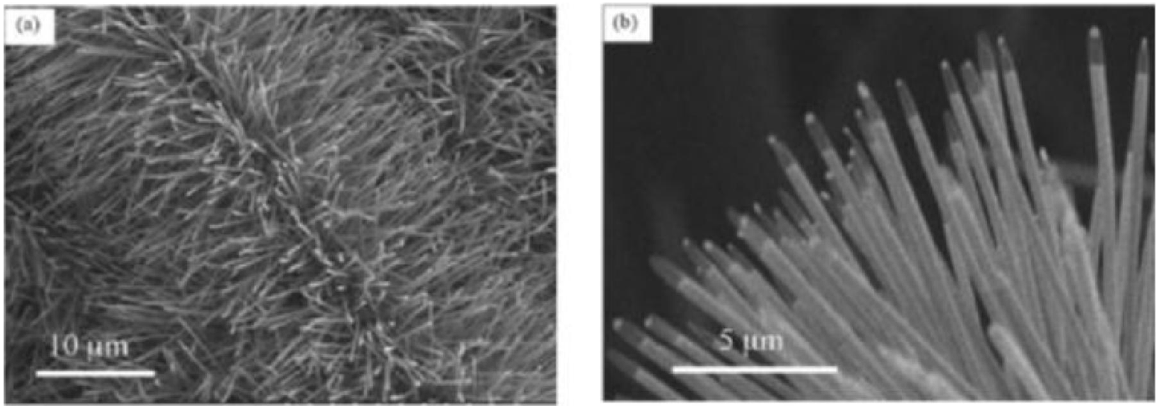

Figure 3 : (a) SEM image showing high coverage of SnC NWs grown on fibers of carbon paper; (b) Higher magnification SEM image showing the tip of nanostructure array[132]

Since metal and metal oxide nanowires have relatively poor corrosion resistance[127,128] it seems that the synthesize nanowires coated with carbon may be good idea to overcome this problem. It has been reported that carbon was coated on Sn or Sn-based oxide nanoparticles to promote their electrochemical performances[129-131]. On this basis Saha et al.[132] reported a three-dimensional core/shell heterostructure, consisting of a Sn nanowire core and a carbon nanotube shell (SnC), was grown directly onto the carbon paper backing. Compared with the conventional Pt/C catalyst layer, the SnC nanowire-based CL showed a higher oxygen reduction performance and excellent stability in a fuel cell environment. The results demonstrated that the core/shell nanowire-based composites were very promising supports in making cost-effective electrocatalysts for CLs in fuel cell applications. Figure 3 shows the SEM images of the SnC NWs grown on a commercially available carbon paper backing used in fuel cell applications. In respect to performance improvement by this unique structure Figure 4a shows the single cell performance of the MEA made with Pt/SnC NW/carbon paper composite electrode as the cathode and standard E-TEK electrode as the anode for H_2/O_2. For comparison, the polarization curve of the conventional

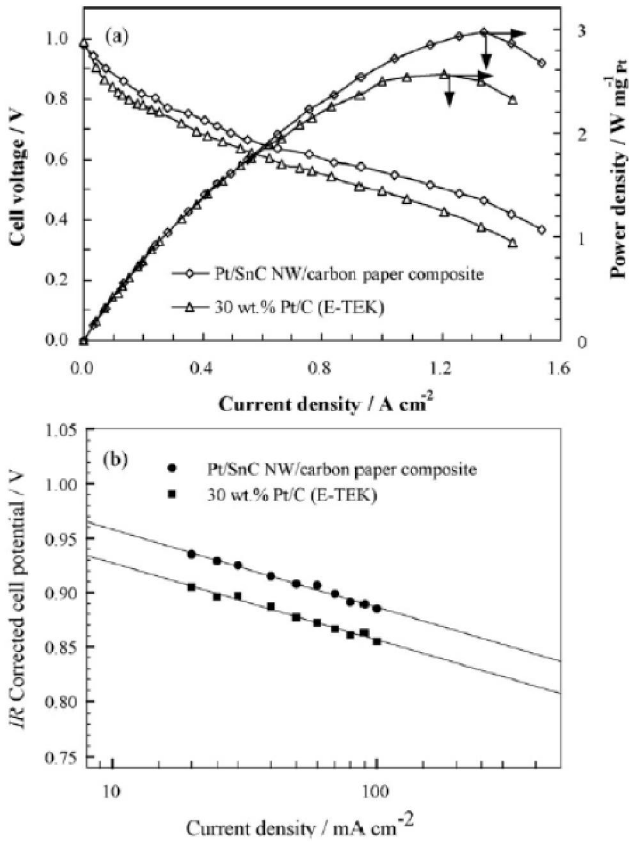

Figure 4 : (a) Comparison of single cell performance of MEAs made with Pt/SnC NW/carbon paper composite (0.21mgPt / cm2) and conventional Pt/C electrode (0.20mgPt /cm2) as cathodes for H2/O2 at 80 °C, Nafion 112 membrane, 25/30 psig anode and cathode back pressure, respectively. Anodes were E-TEK gas diffusion electrode with a Pt loading of 0.5mgPt/ cm2; (b) Comparison of the iR-free Tafel plots for oxygen reduction reaction[132]

MEA made with two E-TEK electrodes is also presented. Polarization characteristics were compared at 80 °C with 25/30 pisg backpressure for the anode and cathode, respectively (100% humidification condition). As seen in Figure 4 a, the MEA made with Pt/SnC NW/carbon paper composite electrode shows higher performance compared to that conventional E-TEK MEA throughout the whole potential range. Comparison of the iR-free Tafel plots for oxygen reduction is presented in Figure 4 b. The mass activity (current density normalized on the basis of Pt loading) at 900 mV (activation-controlled region) for the Pt/SnC NW/carbon paper composite is 308.6 mA /mg Pt, which is 2.5 times higher than the value of 121.0 mA/mg Pt for the Pt/C electrode, indicating a higher activity toward oxygen reduction at Pt/SnC NW/carbon paper composite. According to authors this improvement attributed to the higher dispersion of Pt nanoparticles on the surface of SnC NWs as well as the unique 3D structure of Pt/SnC NW/carbon paper composite. Moreover, the improved performance and power density are achieved at higher current density region using the Pt/SnC NW/carbon paper composite. The improvement at higher current density region clearly indicates a better mass transport for the Pt/SnC NW/carbon paper composite electrode. The power density of a Pt/SnC NW/carbon paper composite electrode and Pt/C electrode, both were normalized to the Pt loading at 0.6 V, were 2.14 and 1.70 W/mg Pt, respectively, showing an improvement of about 0.44W/mgPt in power density for the Pt/SnC NW/carbon paper composite electrode. They also evaluated the stability of SnC NWs on carbon paper (before Pt nanoparticles deposition) by immersing the composite electrode in 0.1 M H_2SO_4 solution over a period of 1500 h at 50 °C. After the test, TEM observations of the composite indicated that SnC NWs was still on the surface of carbon fibers with same density, diameter, and length. Further TEM inspection showed that both the tin core and carbon shell remained original morphology. Therefore these results suggest that the adhesion of SnC NWs to the carbon paper is strong and the stability of SnC NWs is high.

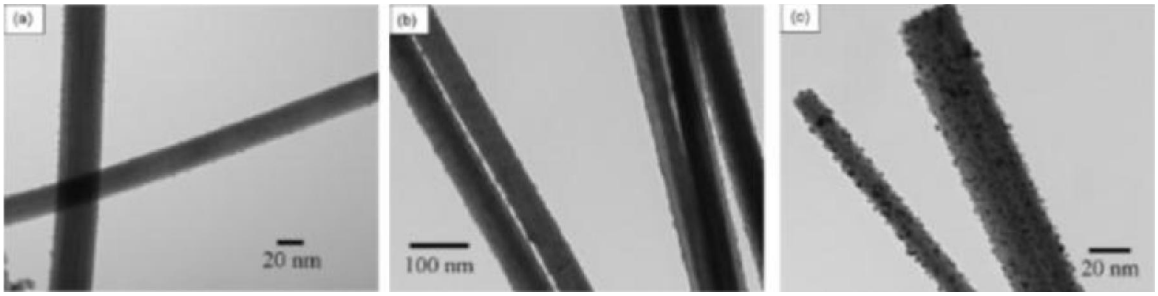

Figure 5 : TEM images of Pt nanoparticles deposited on theW18O49 NWs/carbon paper from different concentrations of Pt precursor (a) 1mM, (b) 2mM and (c) 4mM in glacial acetic acid. The corresponding Pt loadings on the NWs are 0.08, 0.17 and 0.31mg/cm2[133].

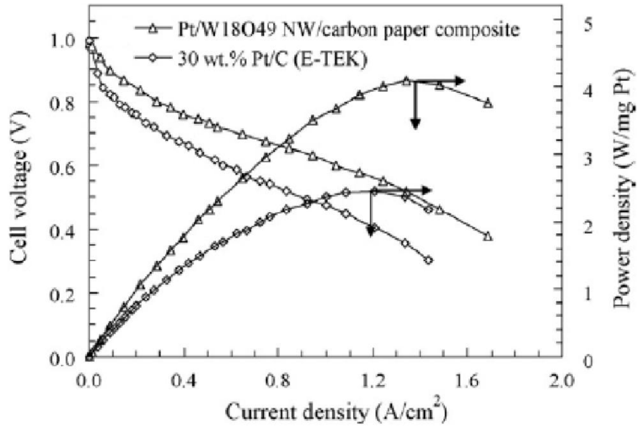

Figure 6 : Polarization curves and power density curves in single cell PEMFC of MEA's made with Pt/W18O49 NW/carbon papercomposite (0.17mgPt /cm2) and conventional Pt/C electrode (0.20mgPt/ cm2) as cathodes for H2/O2 at 80 °C, Nafion 112 membrane,25/30 psig anode and cathode back pressure, respectively. Anodes were E-TEK gas diffusion electrode with a Pt loading of 0.5mgPt /cm2[133]

On the use of tungsten oxide nanostructure material as support again Saha and coworkers[133] reported directly grow $W_{18}O_{49}$ NWs on fuel cell backings as fuel cell catalyst supports to build three-dimensional (3D) electrode structures. This time the Pt nanoparticles were deposited on $W_{18}O_{49}$ NWs/carbon paper by reduction of Pt precursor with glacial acetic acid. Well-dispersed Pt nanoparticles, with a size distribution from 2 to 4 nm, were observed on the surface of $W_{18}O_{49}$ NWs by TEM studies Figure 5. In comparison to conventional Pt/C electrocatalyst, the Pt/ $W_{18}O_{49}$ NW/carbon

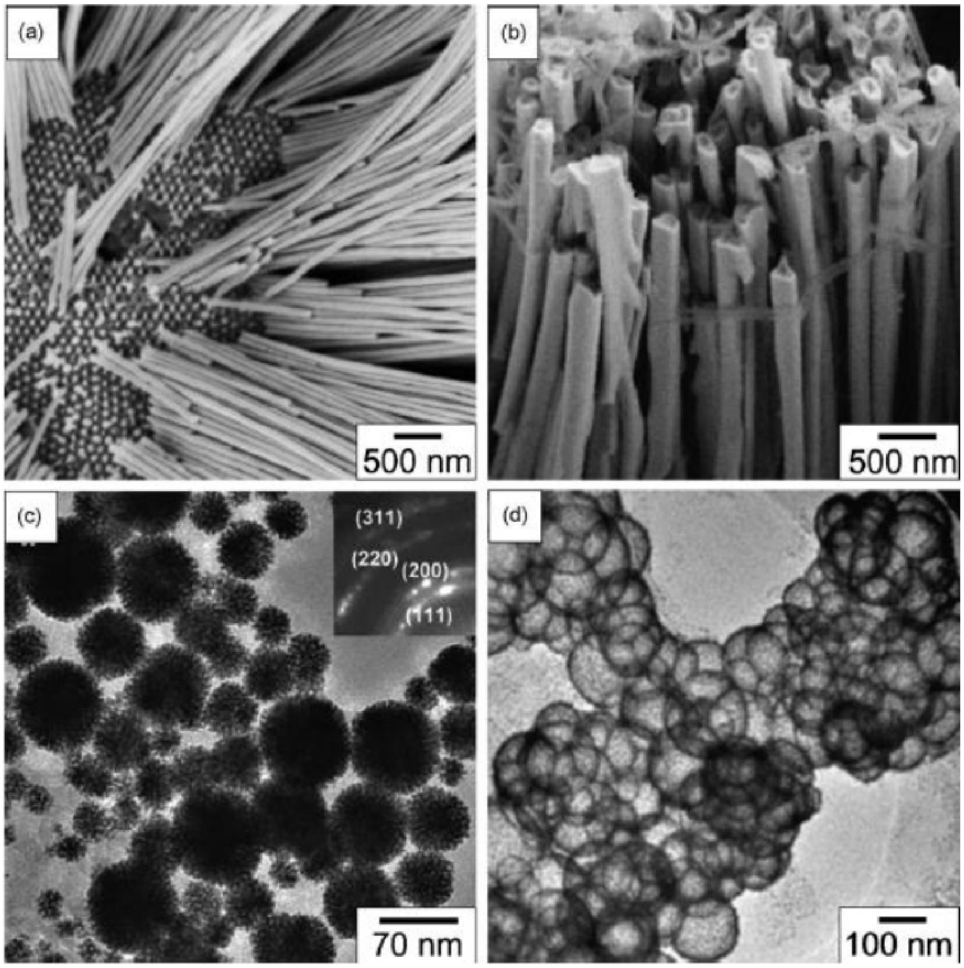

Figure 7 : Representative TEM images of Pt nanostructures with shapes of (a) wire [134], (b) tube [135], (c) dendrite [143], and (d) cage[144], by using templates during synthesis

TABLE 1 : Theoretical Pt loadings of Pt/S89M72BP[224]

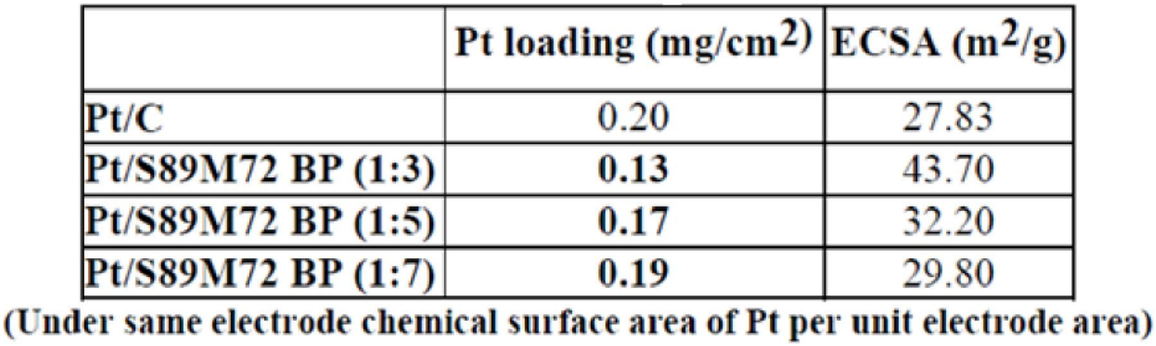

	Pt loading (mg/cm^2)	ECSA (m^2/g)
Pt/C	0.20	27.83
Pt/S89M72 BP (1:3)	0.13	43.70
Pt/S89M72 BP (1:5)	0.17	32.20
Pt/S89M72 BP (1:7)	0.19	29.80

(Under same electrode chemical surface area of Pt per unit electrode area)

TABLE 2 : Characterization of Pt/CeW18O49 NWs/carbon paper and commercial 30 wt.% Pt/C electrodes[134]

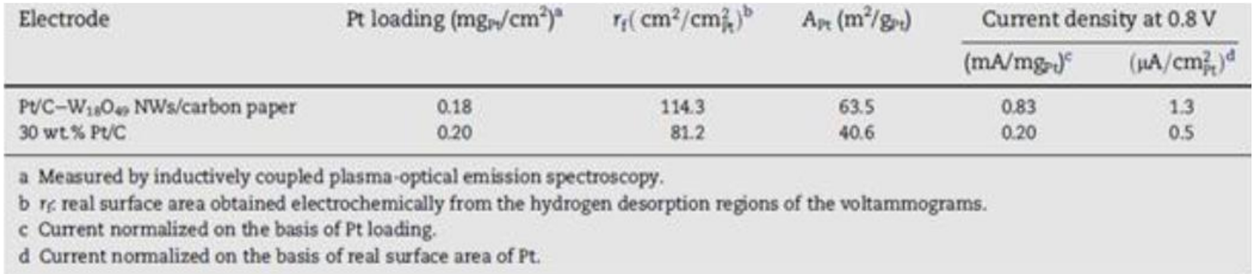

Electrode	Pt loading (mg$_{Pt}$/cm^2)^a	r_f (cm^2/cm$^2_{Pt}$)^b	A_{Pt} (m^2/g$_{Pt}$)	Current density at 0.8 V	
				(mA/mg$_{Pt}$)^c	(μA/cm$^2_{Pt}$)^d
Pt/C–$W_{18}O_{49}$ NWs/carbon paper	0.18	114.3	63.5	0.83	1.3
30 wt.% Pt/C	0.20	81.2	40.6	0.20	0.5

a Measured by inductively coupled plasma-optical emission spectroscopy.
b r_f: real surface area obtained electrochemically from the hydrogen desorption regions of the voltammograms.
c Current normalized on the basis of Pt loading.
d Current normalized on the basis of real surface area of Pt.

paper composite exhibited higher electrocatalytic activity toward the oxygen reduction reaction and better CO tolerance in a single cell polymer electrolyte membrane fuel cell and the Pt/ $W_{18}O_{49}$ catalyst gave roughly 4-fold higher current than the Pt/C reference for nearly the same Pt loading. In terms of activity per mass of Pt at 900 mV, the Pt/ $W_{18}O_{49}$ catalyst gave 0.63 Amg_{Pt}^{-2} vs. the 0.13 Amg_{Pt}^{-2} for the Pt/C reference in this work. According to authors the enhancement in the activity for oxygen reduction on Pt/ $W_{18}O_{49}$ NWs/carbon paper composite is attributed to the uniform dispersion of smaller Pt particles, an improved catalyst-support binding and a synergistic effect of $W_{18}O_{49}$ NWs as catalyst support Figure 6.

In another report, Saha and coworkers[134] extended their previously study by carbon coating the tungsten oxide nanowires grown directly on carbon fiber of a carbon paper by chemical vapor deposition method and Pt nanoparticles were deposited on the nanowires (Pt/C- $W_{18}O_{49}$NWs/carbon paper) to form the composite electrode. The electrocatalytic activities of these composite electrodes for oxygen reduction reaction (ORR) were investigated and the Pt/C- $W_{18}O_{49}$ NWs/carbon paper composite has the mass specific surface area (m^2/gPt, TABLE 2) of 63.5, about 36% higher than that of the commercial Pt/C electrode (40.6 m^2/gPt).

Synthesis of Pt nanostructures

Both chemical and physical templates have been used in producing platinum nanostructures, usually in polycrystalline forms. These templates offer confined spaces and/or functionalized structures for the growth of platinum. There are two major categories: hard and soft templates. The commonly used hard templates, which are composed of spatially well-defined physical structures, include anodic aluminium oxide (AAO)[135-137], mesoporous silica[138], and lithographically patterned templates[139]. By electrodepositing Pt metal into the AAO membranes followed by removal of these hard templates, Pt nanowires could be produced Figure

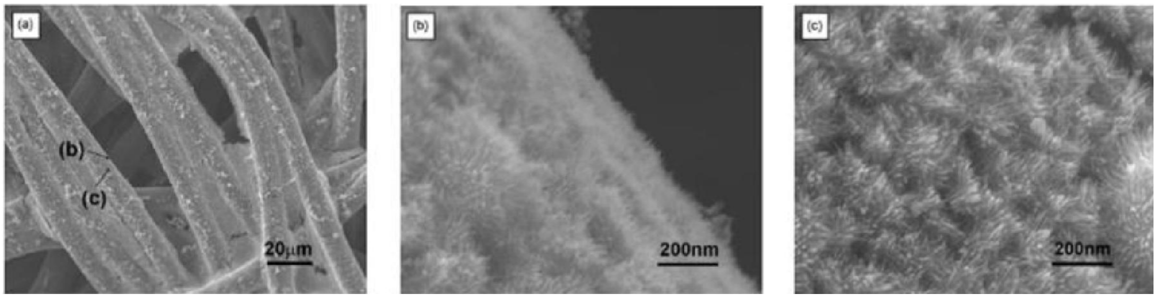

Figure 8 : SEM images of carbon fibres in the carbon paper in situ coated with Pt nanowires[157]

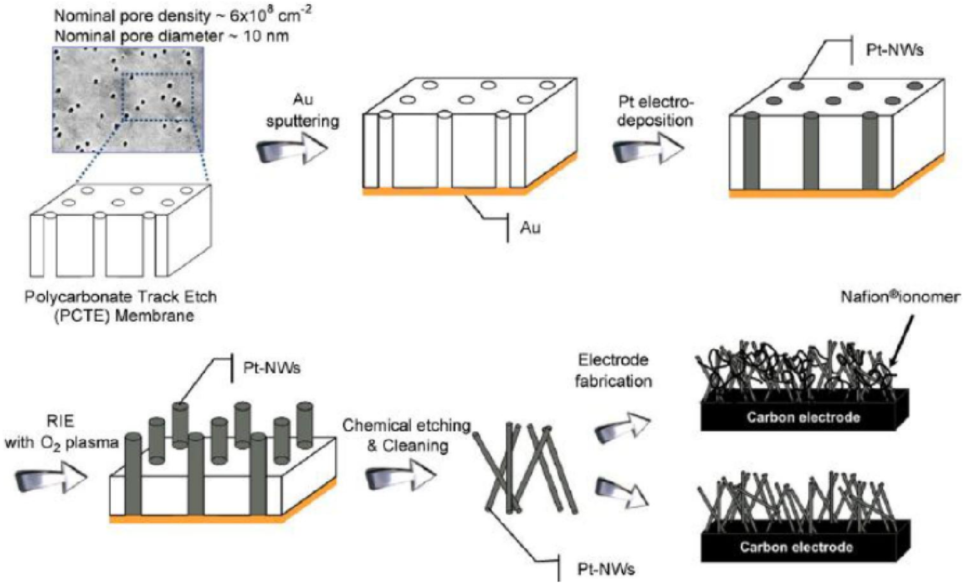

Figure 9 : Schematic illustration of the experimental procedure for the Pt nanowire preparation from the PCTE template membrane to the working electrode fabrication for CV measurements[158]

7a[136]. A further surface modification of the AAO membranes before electrodeposition can lead to the formation of Pt nanotubes, as shown in Figure 7 b[137]. The soft templates include those self-assembled and selforganized structures in solution, such as micelle, reverse micelle, microemulsion, and liposome. Surfactant molecules which have hydrophilic heads and lipophilic long carbonchains are commonly used. They are used in the synthesis of higher-ordered Pt nanostructures, such as dendrites and cages[140]. Platinum nanorods have been produced from crystalline complexes containing both CTA$^+$ and Pt(II) species in the presence of cetyltrimethylammonium bromide (CTAB)[141]. A range of sheet-like and three-dimensional textured Pt nanostructures have been generated by using liposomes as templates Figure 7c-d[142-145].

Pt nanowires and composited hybrid electrocatalyts of Pt-based nanoparticles and nanowires for low temperature polymer electrolyte fuel cells

Pt nanowires

Up to now, highly-dispersed Pt-based nanoparticles (NPs) having approximately 2–3 nm on carbon supports have been used as the state-of-the-art electrocatalysts with advantages of high EAS and large 3-phase boundaries (gas–electrolyte–catalyst) in the fuel cells[146]. Nevertheless, even the highly optimized electrocatalytic system using the Pt-based NPs still offers large opportunities to mitigate impediment of mass transport and decrease charge transfer resistance in the electrodes where a number of interfaces are present between NPs each other or between NPs and polymeric binders[147]. Moreover, nano-sized particle morphologies have high surface energies, thereby inducing to agglomeration of the NPs during electrode reaction. Thus, one-dimensional (1D) nanostructures, i.e., rods, tubes, and wires, of platinum would be recognized as a new promising electrode catalyst for improving the performance of the PEMFCs due to several favorable features resulting from their shape anisotropy on the electrochemical oxidations at electrodes.

Recently, there have been several reports[136,148-152] that demonstrated the Pt or Pt-based nanowires as the electrocatalysts for the methanol oxidation; for instance, Pt and Pt–Ru nanowire array electrodes prepared by electrodeposition over an anodic alumina oxide (AAO) template on Ti/Si substrate[148] and Pt–Ru nanowire network synthesized in a SBA-15 silica template[149]. Pt nanowires formed directly in a Nafion membrane via electrodeposition was also reported and the mass-based activity was compared per gram of Pt between the nanowire and nanoparticle morphology using a single Pt loading of approximately4mg/cm^2[153].

Xia and co-workers have directly grown Pt nanowires on Pt or W gauze by a polyol process in the presence of Fe^{2+} or Fe^{3+} and poly(vinyl pyrrolidone) (PVP). The products indicated a higher tolerance to CO-like intermediates and showed a great activity toward methanol oxidation. However, this method needed a high temperature of 110 °C with surfactant and polyol as solvent[154]. Recently, Sun and co-workers developed a facile wet-chemical method to grow single-crystalline Pt nanowires on the nanospheres of a carbon black via a simple chemical reduction of hexachloroplatinic acid (H_2PtCl_6) with formic acid (HCOOH) at room temperature in aqueous solution. Such Pt nanowire/C nanocomposites showed an improved catalytic activity for the oxygen reduction reaction (ORR) compared with a conventionally Pt/C catalyst made of Pt nanoparticles[147]. The method has also been used to synthesize 3D flower-like platinum nanostructures on carbon paper[155], or to prepare urchin like Pt nanoelectrocatalysts at 30 C in the presence of PVP[156].

By a minor modification of facile formic acid method, Du[157] demonstrated a very simple and effective wet-chemical route to prepare GDEs for PEMFCs, by growing Pt nanowires in situ on GDLs, which were performed by simply immersing carbon paper in a mixed solution of hexachloroplatinic acid, formic acid and PVP at room temperature in aqueous solution. The as-prepared GDEs were used as cathodes and tested in 25 cm^2 PEMFCs fed by hydrogen/air. Figure 8 shows the SEM images of the surface morphology of the Pt/carbon paper integrated GDE. As it can be seen the packed nanowire arrays were densely grown on the fiber surface, with a length of 100–150 nm and a diameter of a couple of nanometers.

Choi et.al[158] prepared platinum nanowires via a template-synthesis method by electrodeposition of platinum within pores of a track-etched polycarbonate

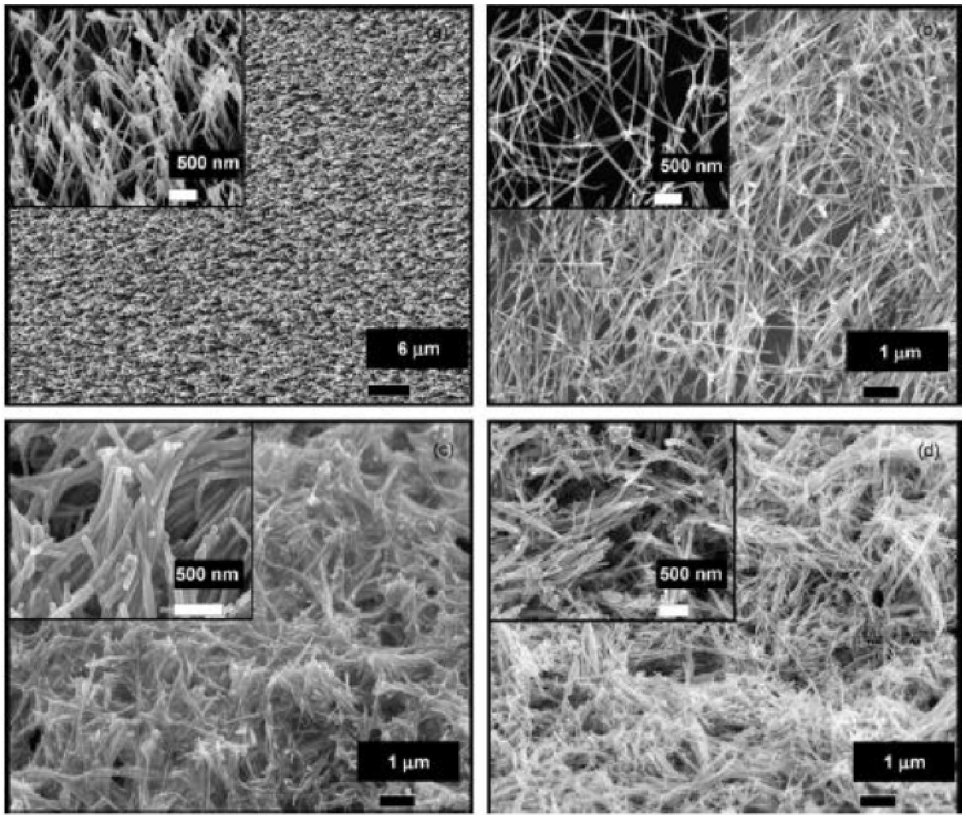

Figure 10 : FESEM images of the Pt nanowires embedded in the PCTE after RIE (a), the Pt nanowires present on Si substrate after separated from the polymer membrane by chemical etching (b), and the impregnated Pt nanowires on the glassy carbon substrate with (c) and without Nafion® ionomer (d)[158]

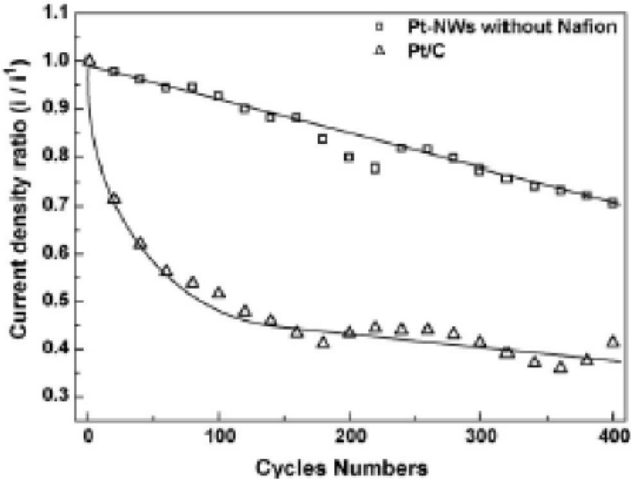

Figure 11 : The long-term cycle stability of Pt/C and Pt-NWs electrodes in 0.5M H2SO4 +2M CH3OH electrolyte solution at a scan rate of 30Mv/s1. The Pt loadings were *ca.* 3mg/cm2[158]

(PCTE) membrane Figure 9, which has advantages in that the polymer template could be easily removed and cleaned without contaminating and morphologically changing the nanowires formed, followed by chemical etching to separate the Pt nanowires from the polymer.

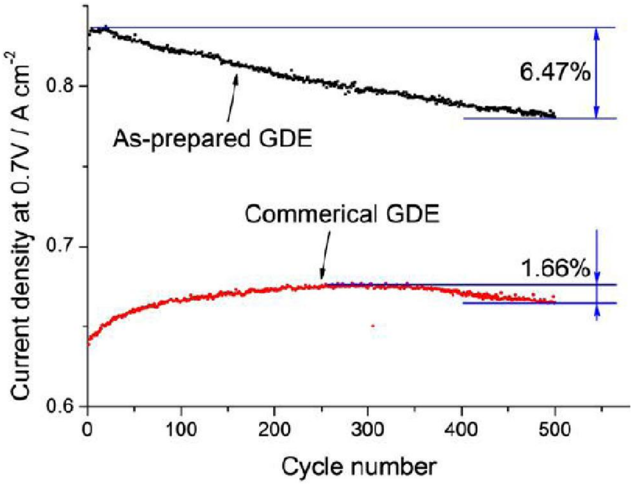

Figure 12 : Degradation plots shown by the current densities at 0.7 V in each voltage scan cycle versus cycle numbers for both types MEAs with (a) the commercial cathode GDEs of E-TEK ELAT GDE LT 120E-W and (b) the as-prepared cathode GDEs with in-situ grown Pt nanowires[159]

They investigated the electrochemical activities of the Pt nanowires for the hydrogen and methanol oxidation by cyclic voltammetry (CV) measurement, which were compared per unit gram of the Pt with those of the commercial 40 wt% Pt/C and high surface area Pt black revealing a polycrystalline phase with nanowire dimension up to 6 μm long and *ca.* 47±9.8 nm of diameter. In their experiments the unsupported Pt nanowires showed the better electrochemical mass activities over the methanol electro-oxidation than supported or unsupported Pt nanoparticles under the high Pt content-loaded conditions that is normally required for direct methanol fuel cells. This enhancement ascribed to its unique physicochemical and electrical properties resulting from the intrinsic anisotropic one-dimensional (1D) nanostructure, such as charge transfer facilitation by reducing number of particle interfaces and more efficient use of Pt by lessening fraction of embedded catalysts. Field-emission scanning electron microscopy (FESEM) taken over the Pt nanowires as shown in Figure 10. Figure 11shows the long-term cycle stability of the Pt nanowire and Pt/C catalysts, which was investigated in the 0.5M H_2SO_4 +2M CH_3OH aqueous solution.

Recently Du and coworkers[159] investigated the effect of varying Nafion ionomer loadings coated on the surface of gas diffusion electrodes (GDEs) with in-situ grown single crystal Pt nanowires and their durability in PEMFCs. In their experiments GDEs were fabricated by growing Pt nanowires directly onto the gas diffusion layer (GDL) surface with a simple one step wet chemical approach at room temperature. The samples were then coated with various Nafion ionomer loadings and examined as cathodes in a 25 cm^2 PEMFC hardware with Hydrogen/Air. The data were compared to commercial GDEs. Performance evaluations showed that the as-prepared GDEs with Pt nanowires required higher Nafion ionomer loading coating compared to the commercial ones. Accelerated ageing tests (500 cycles of voltage scan) were performed in views of evaluating the as-prepared GDE durability. The experimental data showed that the as prepared GDEs exhibited much larger current densities at 0.7 V (where the Nafion ionomer loading coating for the commercial and the as-prepared GDEs are 0.9 mg/ cm^2 and 1.2 mg/cm^2 respectively) but higher degradation rates compared to commercial GDEs, indicating that the as-prepared GDEs gave poor durability Figure 12. According to authors this was due to the difference in GDE surface nanostructures influenced by the electrolyte ionomer loading coating. A schematic illustration of the Nafion ionomer coating on the GDE surface, based on the MEA measurement and SEM results in order to understand the mechanism of this effect of electrolyte ionomer loadings on the GDE performance is presented in Figure 13. This effect is further discussed in their paper.

Nanowires versus nanoparticles

Zhou et.al[160] showed that the morphology of nanostructured Pt catalysts affect significantly the kinetics of various reactions. Their report was on a pronounced morphology effect in the electrooxidation of ethanol and carbon monoxide (CO) on Pt nanowires and nanoparticles in an acidic solution. The high resolution transmission electron microscopy analysis in their devoted study showed the intrinsic morphology difference between these two nanostructured catalysts. Voltammetric and chronoamperometric studies of the ethanol electrooxidation revealed that these nanowires had a higher catalytic activity by a factor of two relative to these nanoparticles Figures 14,15. The rate for CO monolayer oxidation exhibits similar morphology-dependent behavior with a markedly enhanced rate on the Pt nanowires. The morphology-induced change in catalytic activity and selectivity in ethanol electrocatalysis is discussed in detail in related paper. Theyrecorded all current data after the catalysts were immersed at 0.07 V under potential control and then stepped to reaction potentials. Currents are normalized to the measured Pt surface area.

Composited hybrid of Pt NPs and NWs

One-dimensional (1-D) nanostructures such as nanowires (NWs) have been demonstrated as new electrocatalysts to overcome the weaknesses of NPs in fuel cell electrodes[161-164]. The nanowire electrocatalysts can provide numerous advantages like: (i) supplying facile pathways for charge transfer with a high conductivity of anisotropic NWs, (ii) reducing embedded sites of electrocatalysts from the continuously-connected 1-D nanostructure, and (iii) facilitating effective mass transfer by networking the anisotropic morphology. In spite of such qualities, the nanowire structured electrocatalysts have still suffered from much smaller specific surface area than supported NPs. Therefore, if the NPs and NWs can be effectively

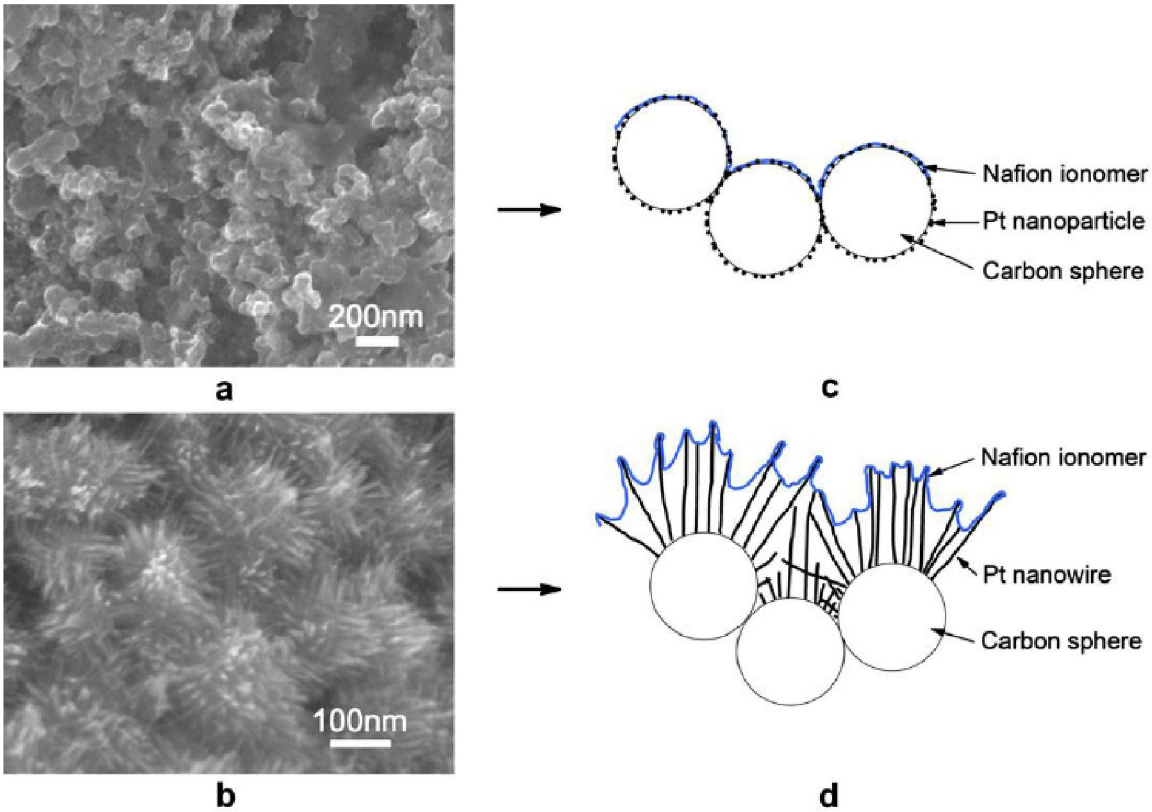

Figure 13 : SEM images and schematic illustration of the Nafion ionomer chain coated on the surface of the commercial cathode GDEs of E-TEK ELAT GDE LT 120E-W with commercial spherical catalyst nanoparticles ((a) and (c)) and the as-prepared cathode GDEs with in-situ grown Pt nanowires ((b) and (d))[159]

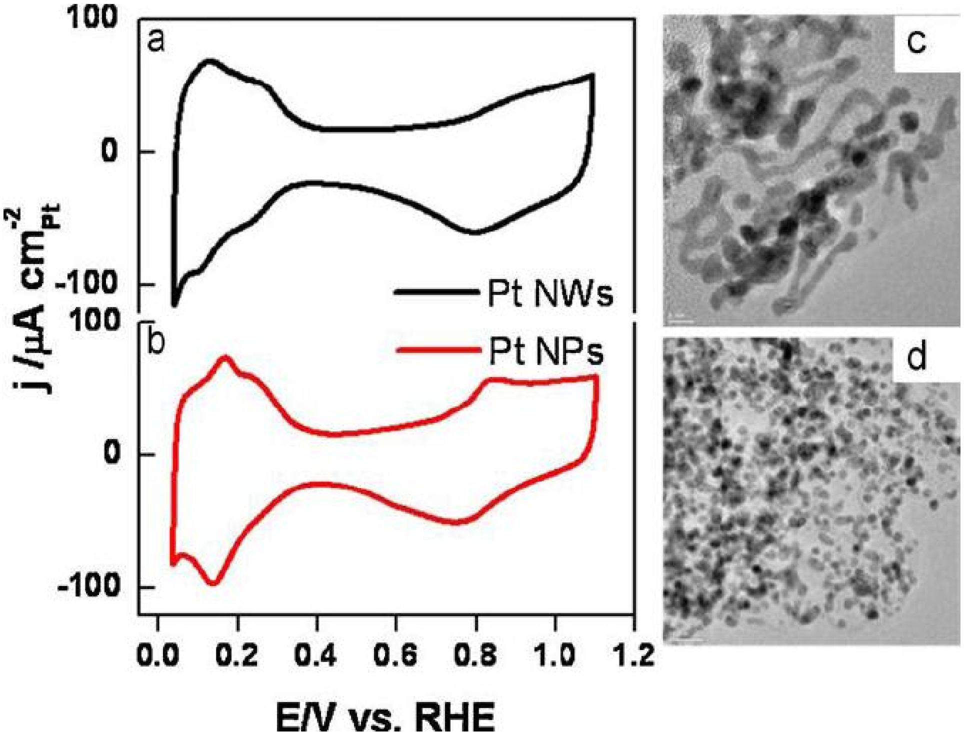

Figure 14 : Voltammetric curves for (a) Pt nanowires and (b) Pt nanoparticles in 0.1 M HClO4 solution. Scan rate: 50 mV/ s1. Currents are normalized to the measured Pt surface area (Hads charge after double layer correction). Typical HRTEM images are highlighted of Pt nanowires (c) and Pt nanoparticles (d)[160]

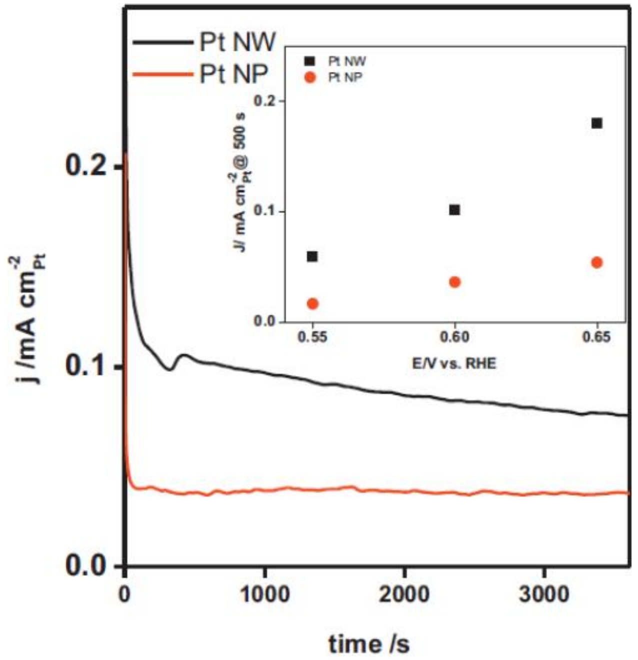

Figure 15 : Comparison of current–time plots for ethanol oxidation activity on Pt nanowires (black) and nanoparticles (red) in 0.2 M ethanol in 0.1 M HClO4 solution at 0.65 V for 3600 s reaction time. Inset shows comparison of current densities measured at three different potentials (0.55 V, 0.60 V and 0.65 V) at 500 s reaction time[160]

composited to strengthen the advantages but alleviate the disadvantages of both nanostructures, the fuel cell performance could be considerably improved.

Kim et.al[165] reported a new and highly improved electrocatalytic system of a composited hybrid electrode with Pt-based nanoparticles (NPs) and nanowires (NWs) for low temperature polymer electrolyte fuel cells. Pt based NWs have been take in as an option that can provide facile charge transport with a high activity for oxidation of fuels, for overcoming the disadvantages of Pt-based NPs as the state-of-the-art electrocatalysts. A special electrode structure like grid using the anisotropic morphology of Pt-based NWs can also supply efficient mass transport and moderate inept use of Pt by reducing embedded catalyst particles. Herein, they demonstrated that an advanced and very efficient hybrid structure of electrode, composited with highly-dispersed Pt-based NPs and NWs, shows significantly improved performances both in the CH_3OH-fueled and H_2-fueled fuel cells through synergistic effects by assimilating advantages of two different morphologies.

Figure 16 shows scanning electron microscopy (SEM) images of a commercial Pt NPs catalyst supported on carbon, Pt NWs catalyst, and hybrid Pt NPs/NWs. These images represent their actual morphologies after they are loaded onto carbon paper as an anode electrode for the fuel cell.

The single fuel cell performances evaluation over

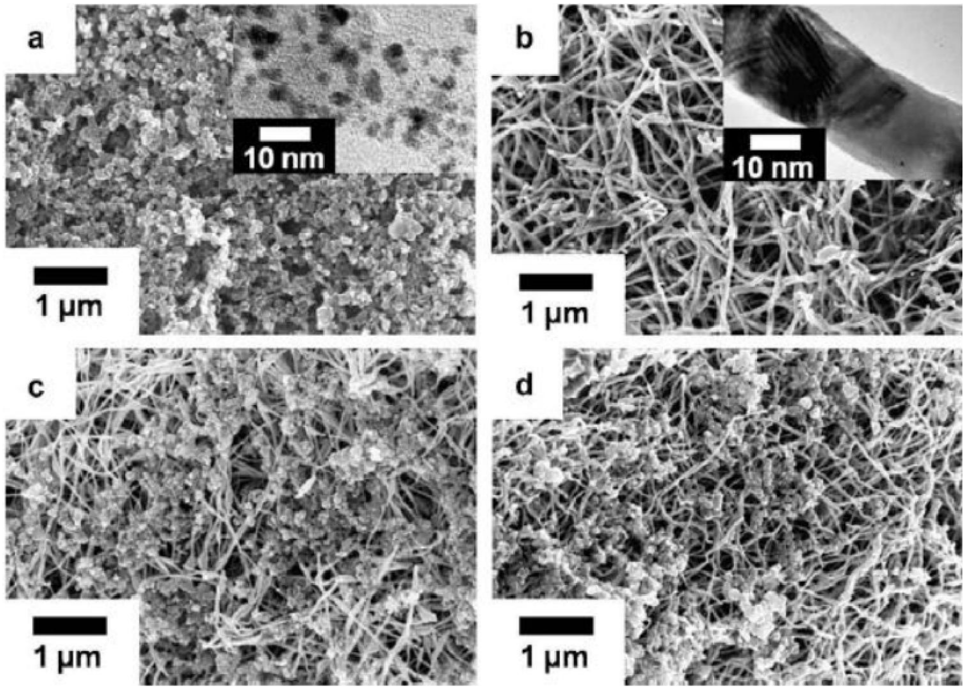

Figure 16 : SEM images of (a) supported Pt NPs on carbon, (b) Pt NWs, (c) hybrid composites of Pt NPs/NWs, (d) hybrid composites of PtRu NPs/NWs on carbon paper; inset figures of (a) and (b) are their TEM images[165]

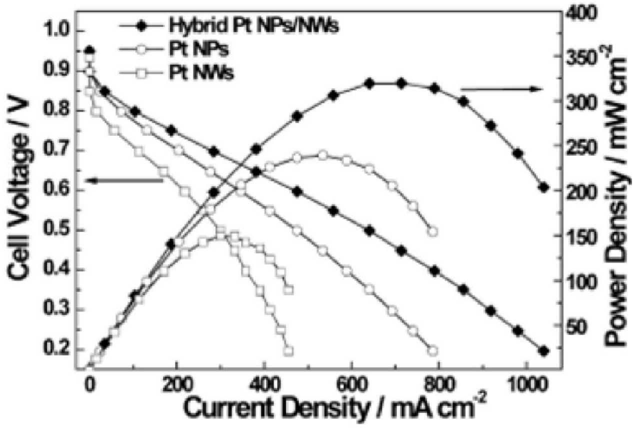

Figure 17 : Polarization curves of H2-fueled PEMFCs using Pt NPs, Pt NWs, and hybrid Pt NPs/NWs (NPs:NWs = 50:50metal wt%)[165]

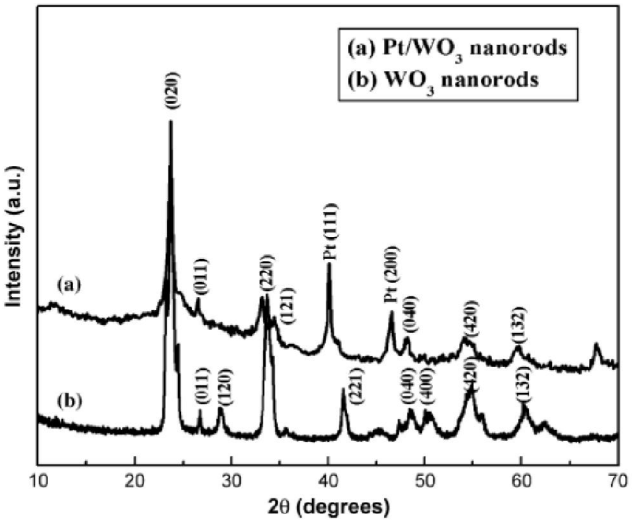

Figure 18 : XRD patterns of (a) Pt/WO3 nanorods and (b) WO3 nanorods[167]

the hybrid composites of Pt-based NPs/NWs were carried out for the actual effects in the anode electrodes after fabricating MEAs. Figure 17 presents the polarization curves over Pt NPs, NWs, and hybrid PtNPs/NWs for PEMFCs with pure H_2 gas at the anode and O_2 gas at the cathode. Although the Pt NPs have a higher maximum power density of ca. 225 mW/cm^2 than that of Pt NWs however, the hybrid composite systems of Pt NPs/NWs electrocatalyst show again a significantly improved maximum power density of ca. 325mW/cm^2, which are higher by at least 50% compared even with the optimum PEMFC catalyst of Pt NPs. The significant enhancements of the single cell performances on PEMFCs, by integrating two different morphologies of nanoparticles and nanowires catalysts, may be achieved via combining their advantages but relieving of their disadvantages like a poor conductivity over NPs and a small active area over NWs. These results evidently demonstrate that the hybrid electrocatalytic system with NWs and NPs could successfully improve the overall performances of low temperature polymer electrolyte fuel cells. The synergistic effects of hybrid structure system are realized on the fuel cell electrodes and demonstrated in the related work.

Nanorods

Recently, one-dimensional (1D) nanorods have attracted remarkable attention owing to their unique properties and potential for various novel applications[166].

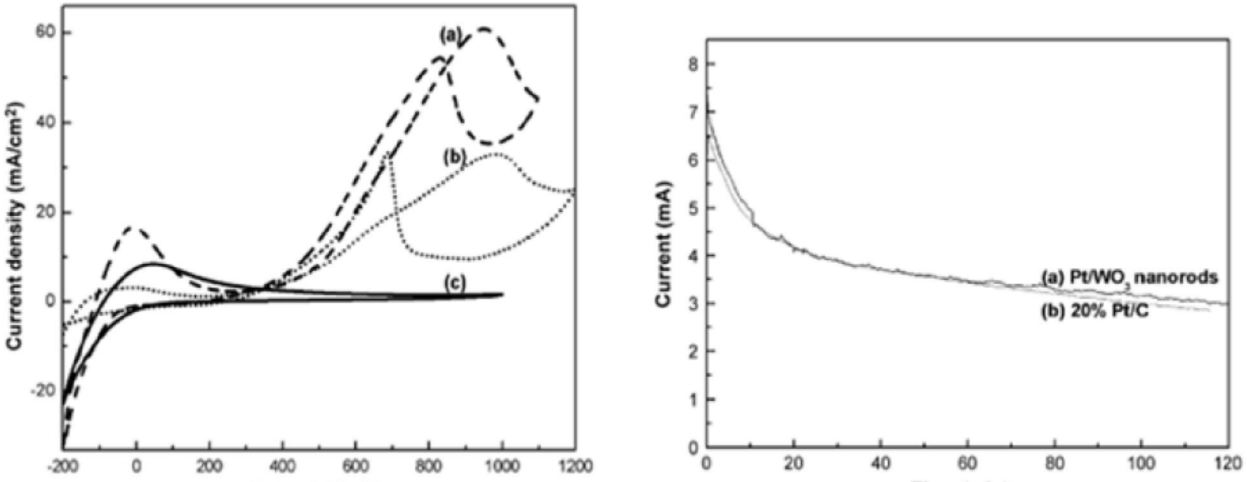

Figure 19 : (A)Cyclic voltammograms of (a) Pt/WO3 nanorods, (b) Pt/C (Johnson Matthey) and (c) WO3 nanorods in 1M H2SO4/1M CH3OH at 50mV/s1.(B) Current density vs. time curves at (a) Pt/ WO3 nanorods and (b) Pt/C (Johnson Matthey) measured in 1M H2SO4 +1M CH3OH. Potential stepped from rest potential to 0.6V vs. Ag/AgCl[167]

Nanorods have large specific surface areas, so metal oxides such as WO_3 in a nanorod form could be an efficient support for fuel cell catalysts. Maiyalagan and Viswanathan[167] synthesized tungsten oxide (WO_3) nanorods from phosphotungstic acid $H_3PW_{12}O_{40}$ in methanol solution using an anodisc alumina membrane as a template by infiltratring the colloidal suspension into the membrane under vacuum by a wetting method and subsequently platinum nanoparticles were supported on the nanorods by conventional impregnation method. The diameter of the nanorods was found to be around 200 nm according to SEM observation. The size of the Pt nanoparticles was in the range of 3–4 nm. The XRD patterns for the as-synthesized tungsten oxide nanorods and platinum-loaded tungsten oxide nanorods are given in Figure 18 (a) and (b), respectively.

A film of Pt/WO_3 nanorods on a glassy carbon electrode exhibits good electrocatalytic activity towards the oxidation of methanol than the commercial Pt/C catalyst by a factor of two Figure 19(A). The chronopotentiometric results of methanol oxidation in 1M H_2SO_4 and 1M CH3OH at 0.6V in the stability measurements are presented in Figure 19(B). The Pt/WO_3 nanorods electrode not only exhibit higher initial activity but are also more stable than the Pt/C electrode. According to authors high electrocatalytic activities and good stabilities are attributed to a synergistic effect between Pt and WO_3 that avoids poisoning of the electrodes.

Rajeswari et al.[168] synthesized WO_3 nanorods by pyrolysis of tetrabutylammonium decatungstate $((C_4H_9)_4N)\ 4W_{10}O_{32}$ at 450 °C. They reported a surfactant directed large-scale synthesis of single crystalline WO_3 nanorods formed by a single step pyrolysis of surfactant encapsulated tungsten oxide clusters. The employed route was template free, contaminant free, easy, economical and required a low temperature for the fabrication of WO_3 nanorods. The proposed mechanism for the formation of WO_3 nanorods is shown in Scheme 20:

$Na_2\ WO_4$ and tetrabutylammonium bromide (TBABr) reacted to form the precursor compound $((C_4H_9)_4N)\ 4\ W_{10}O_{32}$. In the precursor compound, inorganic metal oxide clusters ($W_{10}O_{32}{}^{4''}$) are charge balanced with the surfactant group (TBABr). TBABr controls the irregular arrangement of the metal oxide clusters by providing a steric environment around them. This led to the formation of 1D array of metal oxide clusters. During pyrolysis at 450 °C, removal of the surfactant species ($(C_4H_9)_4N^+$) and decomposition of the $W_{10}O_{32}$ led to the formation of pure, single crystalline WO_3 nanorods. Figure 21a-d shows the high resolution TEM images of nanorods of WO_3 in high yield sand platinum loaded WO_3 nanorods. The dimensions of the nanorods calculated from the TEM images varied in the ranges of 130–480 nm and 18–56 nm of length and width, respectively. And the size of the Pt nanoparticles calculated was in the range of 4–6 nm.The used so-fabricated WO_3 nanorods as supports for platinum nanoparticles (Pt/WO_3 nanorods) in methanol oxidation and the catalytic activity of this system has been compared with that of commercially available Johnson Matthey carbon supported 20% Pt-Ru catalyst (Pt-Ru/C (J.M.)) and bulk WO_3 supported 20% Pt (Pt/bulk WO_3) using electrochemical measurements Figure 22.

Nanotubes and nanofibers

Much of the current interest in nanotubular materials was initiated by the discovery of carbon nanotubes, which are promising for many applications, particularly in the field of fuel cell. Although noncarbonacous nanotubes were identified in the early 1990s, relatively little research has been carried out on their synthesis and characterization. Noncarbonacous nanotubular materials possess unique combinations of physicochemical properties, and are often easier to synthesize than carbon nanotubes. These properties and comparatively low synthesis costs can render noncarbon nanomaterials attractive for technological applications. Nanostructured TiO_2 materials, with a typical dimension less than 100 nm, have recently invented. Such materials include spheroidal nanocrystallite and nanoparticles together with elongated nanotubes, nanosheets, and nanofibers. During the last few years, many reports on physicochemical properties, pointing particular applications, have been published. Bavykin and et.al[169] reviewed the TiO_2 nanostructured materials.

Titanium dioxide, which is well known for its high catalytic activity, stability in acidic or alkaline solutions and non-toxic properties, has been extensively used as

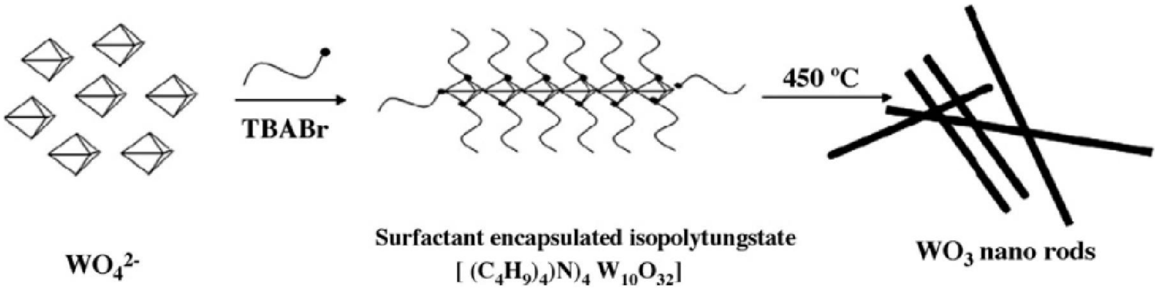

Figure 20 : Fabrication of WO3 nanorods[168]

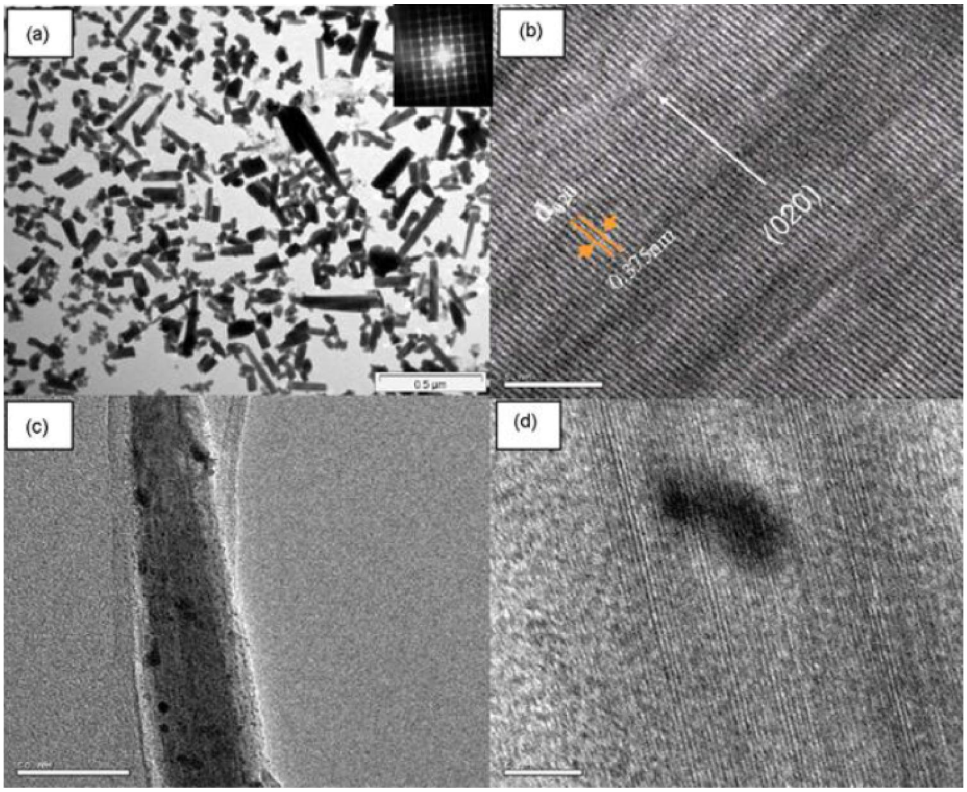

Figure 21 : (a) TEM of WO3 nanorods (inset: an electron diffraction pattern obtained from the WO3 nanorod), (b) HRTEM image of a WO3 nanorod, (c) a low magnification HRTEM image of Pt/WO3 nanorods, and (d) HRTEM image of a Pt nanoparticle on WO3 nanorod[168]

photocatalysts to carry out oxidation of methanol[170-172]. Recently, it had also been demonstrated that Pt–TiO_2/CNTs had higher electro-catalytic activity and CO-tolerance for ethanol oxidation[173]. Titania nanotubes (TNT) prepared from TiO_2 nanoparticles have some pronounced potential as materials with novel properties that are not found in TiO_2 nanoparticles.

Song et.al[174] selected novel titanate nanotubes as the cocatalyst to promote Pt/C (E-TEK; 20 wt.% Pt on Vulcan) catalyst for ethanol electro-oxidation and compared it with Pt/C and TiO_2/Pt/C catalysts in terms of the electrochemical activity for ethanol oxidation using cyclic voltammetry (CV), chronoamperometry and CO stripping voltammetry at 25 °C in acidic solutions. The results demonstrated that the TNT can greatly enhance the catalytic activity of Pt for ethanol oxidation and increase the utilization rate of platinum. The CO stripping test showed that the TNT can shift the CO oxidation potential to lower direction than TiO_2 does, which is useful for ethanol oxidation.

Various methods for the synthesis of TiO_2 nanotubes have been developed in recent years, including anodic oxidation[175,176], template synthesis[177] and hydrothermal synthesis[178]. In respect to their high stability, high surface area and moderate electrical conductivity, titanium dioxide nanotubes (TONTs) have been investigated as fuel cell catalyst support[506–509]. In relation to methanol oxidation and oxygen reduction processes in

DMFCs, Pd and PtRu, and PtNi and PtCo supported on TONTs were investigated for the methanol oxidation reaction (MOR)[179,180] and the oxygen reduction reaction (ORR)[181] respectively.

Macak and coworkers[180] explored oxidative electrocatalytic properties of a system consisting of bimetallic Pt/Ru nanoparticles dispersed over a nanotubular self-organized TiO$_2$ matrix. This nanotubular TiO$_2$ support provided a high surface area and it significantly increases the electrocatalytic activity of Pt/Ru for methanol oxidation. Annealed to anatase, the TiO$_2$ nanotubular support exhibited even higher enhancement effect during electrooxidation of methanol than when used in the "as-formed" amorphous structure. Figure 23 shows SEM images of annealed nanotubular TiO$_2$-layer in the top (a) and cross-sectional (b) views. It is apparent from the images that the TiO$_2$ layer consists of arrays of nanotubes having a length of approximately 500 nm and the average nanotube diameter of 100 nm. The spacing between the tubes is approximately 150 nm, and the wall thickness is about 15 nm.

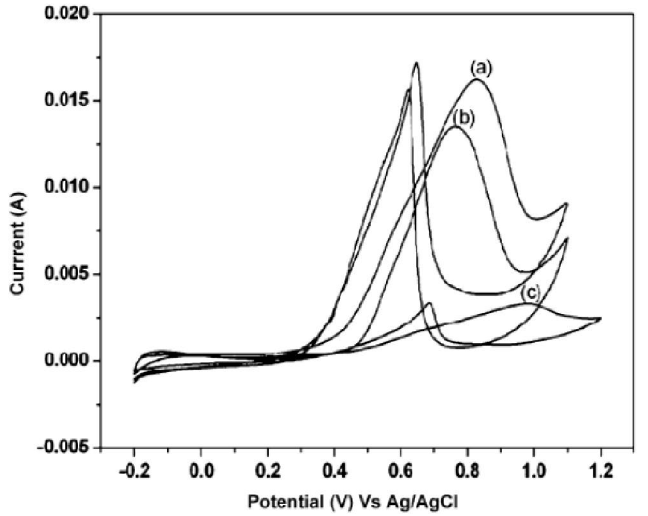

Figure 22 : Cyclic voltammograms of (a) 20% Pt/WO3 nanorods, (b) 20% Pt-Ru/C (J.M.), and (c) 20% Pt/bulk WO3 in 1M CH3OH–1M H2SO4 at a scan rate of 25mV/s[168]

Figure 24 shows cyclic voltammetric and chronoamperometric curves for annealed compact and nanotubular TiO2 in 1 mol/ dm^3 H$_2$SO$_4$ containing 1 mol/ dm^3 CH$_3$OH. As can be seen for the same loading of Pt/Ru nanoparticles and under the same experimental conditions, the voltammetric currents related to the oxidation of methanol are almost seven times higher (at 0.8 V) for the catalyst supported on the nanotubular TiO$_2$ matrix when compared to the system supported on compact TiO$_2$. Accordingly the electrocatalytic currents recorded vs. time (at 0.3 V) under the chronoamperometric conditions are also much higher for nanotubular TiO$_2$ than for the compact TiO$_2$.

Wang et al.[179] investigated the electro-oxidation of methanol in sulfuric acid solution using palladium well-dispersed on titanium nanotubes. TONTs were prepared by the alkaline hydrothermal method reported in elsewhere[182]. HRTEM results show uniform nano-sized TiO$_2$ nanotubes with 10nm in diameters Figure 25.

Pd/TONT catalysts were synthesized at 120 °C using the ethylene glycol reduction method. Pd dispersed on titania nanotubes, which leads to high surface area substrates, showed higher catalytic activity for the MOR than that of pure Pd and Pd supported on TiO$_2$ nanoparticles Figure 26. It is clear that the titania nanotube catalyst is the most active, followed by the nanoparticles and then the pure Pd. The palladium well dispersed on titania tubes with Nafion membrane is the best catalyst because TiO$_2$ nanotubes have a small size in diameter and therefore higher specific surface area inside and outside, which is desirable for the electrocatalyst.

Chen et.al[183] synthesized PtNTs and PtPdNTs (50 nm diameter, 5–20 mm long and 4–7 nm wall thickness) and tested their suitability as catalysts for ORR in PEMFCs. The SEM and TEM images Figure 27 A, B showed the uniform diameter (45 nm), wall thickness

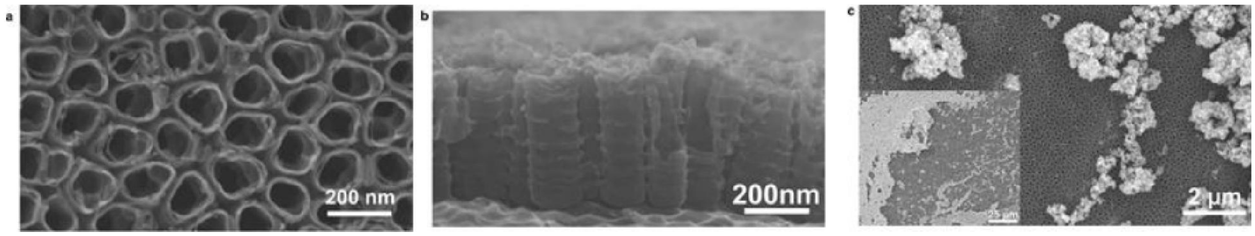

Figure 23 : SEM images of annealed nanotubular TiO2 layer: (a) top-view, (b) cross-sectional view, and (c) top-view following immobilization of Pt/Ru nanoparticles. The inset to figure (c) shows the latter image at low magnification. The cross-sectional image is taken from mechanically cracked sample[180]

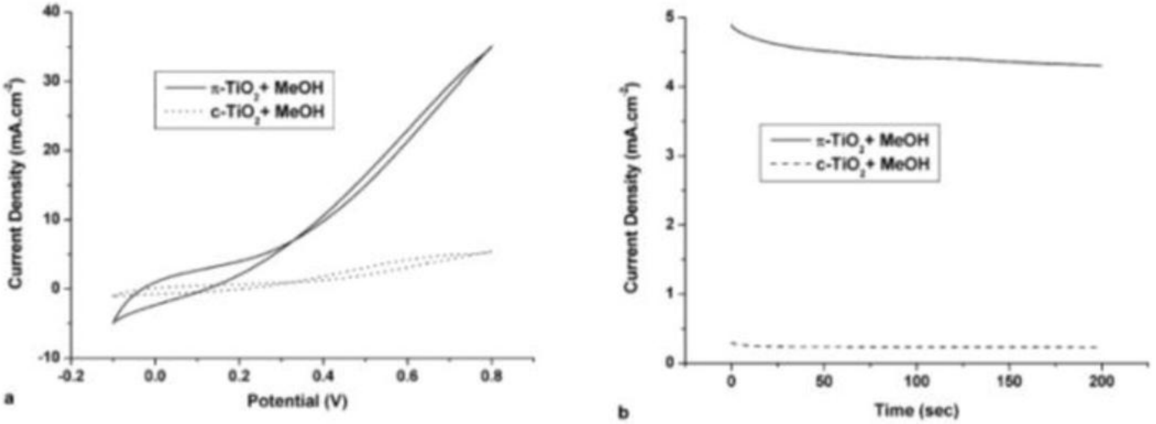

Figure 24 : (a) Cyclic voltammograms recorded for annealed nanotubular (p-TiO2) and compact TiO2 layer (c-TiO2) with Pt/ Ru nanoparticles (loading:1.35 mg) in 1 mol/ dm3 H2SO4 + 1 mol /dm3 CH3OH with a scan rate of 50 mV /s1; (b) chronoamperometric current–time curves recorded at 0.3 V for the corresponding samples[180]

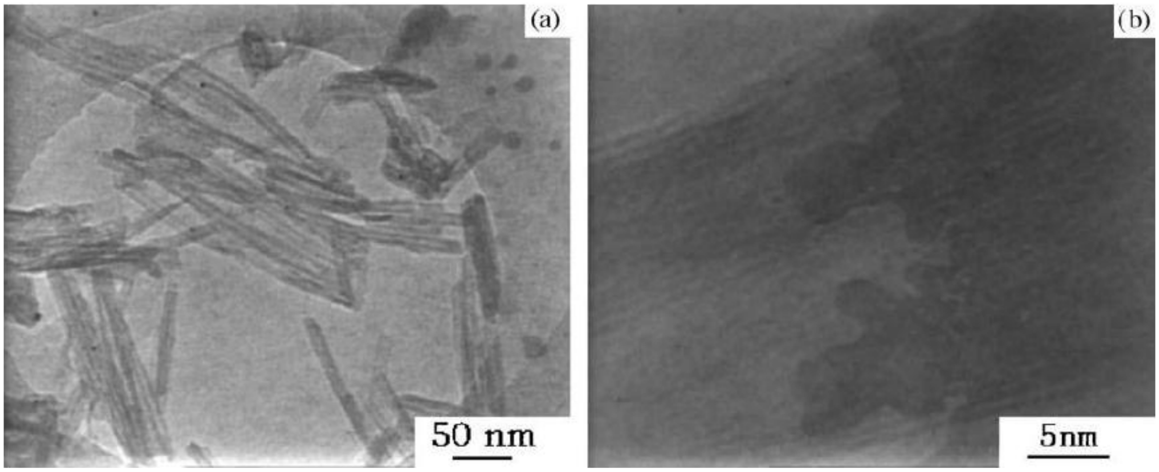

Figure 25 : High-resolution TEM images of TiO2 nanotubes

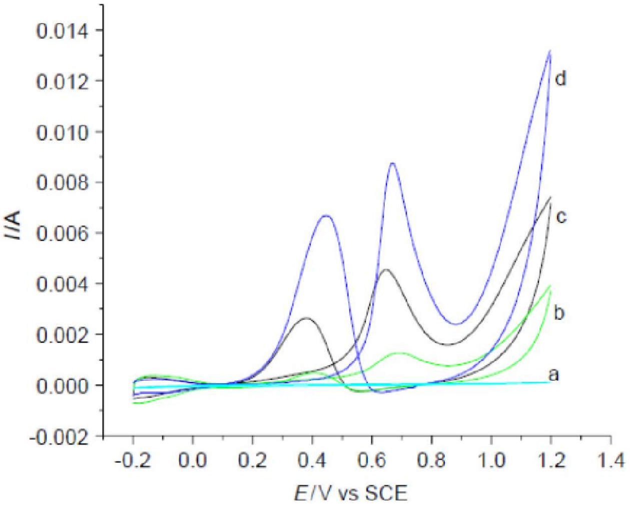

Figure 26 : Cyclic voltammograms in 1M CH3OH+1M H2SO4 for a Pd catalyzed (reduction of PdCl2 by glycol ethanol) TiO2 nanotube dispersed with Nafion solution on Ti: (a) pure TiO2 nanotubes; (b)pure Pd: (c) 3wt% Pd–TiO2 nanoparticles; (d) 3wt% Pd–TiO2 nanotubes. Scan rate 50 mV/s.

(7 nm), and length (10 mm) of the PtPdNTs. The inset of figure 84 B shows an electron diffraction pattern of the PtPdNTs. Their approach to a durable electrocatalyst was to develop supportless platinum nanotubes (PtNTs) and platinum-alloy nanotubes (e.g., platinum–palladium- alloy nanotubes (PtPdNTs)) as the cathode catalyst. Because of their unique combination of dimensions at multiple length scales, PtNTs and PtPdNTs can provide high platinum surface area by their nanometer-sized wall thickness without the need for a high-surface-area support (e.g.,carbon black). They performed durability tests by cycling the electrode potential between 0 and 1.3 V versus a reversible hydrogen electrode (RHE) at a scan rate of 50 mV/s in an argon purged 0.5 m H_2SO_4 solution at 60 °C. The cyclic voltammograms for Pt/C (20 wt% platinum on Vulcan XC-72; E-TEK), platinum black (PtB; E-TEK), and PtNTs showed a significant decrease of platinum

ECSA for Pt/C and little reduction for PtNTs as the number of cycles increases Figure 28 A. The platinum ECSA of the PtNTs only decreases about 20% even after 1000 cycles, while the platinum-black and Pt/C catalysts have lost about 51 and 90% of their platinum ECSA, respectively. The ORR curve Figure 28 B shows that the half wave potential of the PtPdNTs is 0.851 V, which is higher than that of the PtNTs, platinum black, and Pt/C. The mass activity of the PtPdNTs is 1.4 and 2.1 times higher than that of Pt/C and platinum black, respectively, and the specific activity of the PtPdNTs is even 5.8 and 2.7 times higher than that of the Pt/C and platinum-black electrocatalysts, respectively, at 0.85 V.

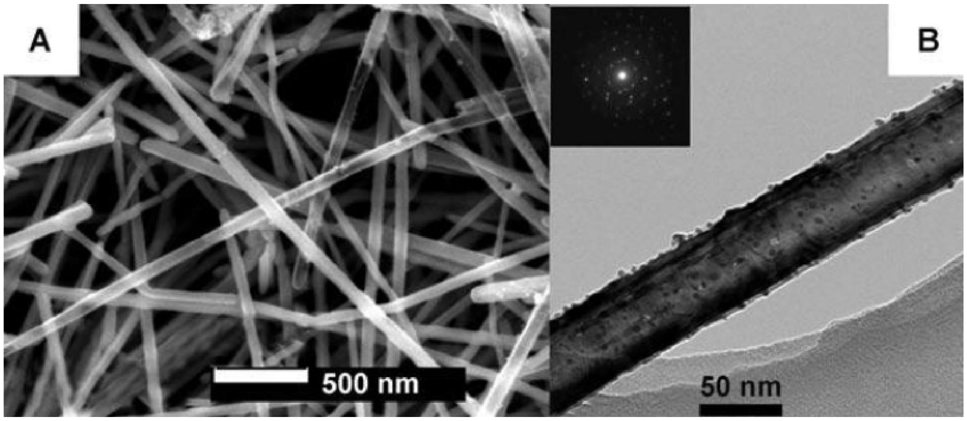

Figure 27 : A) SEM image of PtPdNTs. B) TEM image and electron diffraction pattern (inset) of PtPdNTs[183]

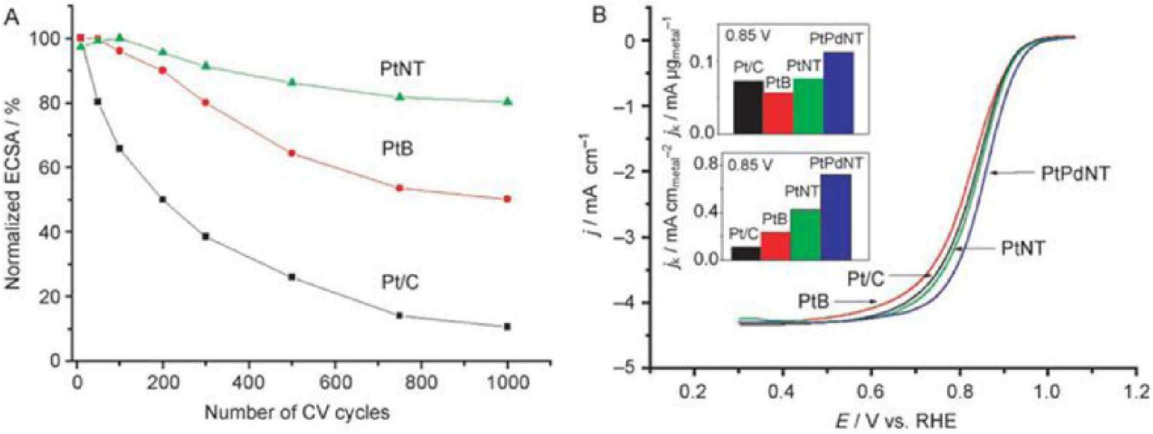

Figure 28 : A) Loss of electrochemical surface area (ECSA) of Pt/C (E-TEK), platinum-black (PtB; E-TEK), andPtNT catalysts with number of CV cycles in Ar-purged0.5 m H2SO4 solution at 60°C (0–1.3 V vs.RHE, sweep rate 50 mV/s). B) ORR curves (shown as current–voltage relations) of Pt/C, platinum black (PtB), PtNTs, andPd PtNTs in O2-saturated0.5 m H2SO4 solution at room temperature (1600 rpm, sweep rate 5 mV/s). Inset: Mass activity (top) andspecific activity (bottom) for the four catalysts at 0.85 V[183]

Nanostrucured conducting polymers (CP) -Supported Pt-based Electrocatalysts: Structure, synthesis, characterization and performance of PEM fuel cell

Conducting polymers (CP) have been extensively studied during the last 20 years in view of their potential application for example as capacitors, sensors, the photo degradation of semiconductor electrodes in galvanic cells, supports for fuel cells or for protection against corrosion, and for other applications. Conducting polymers constitute a class of materials that possess properties of both organic polymers and inorganic conductors or semiconductors[184]. Conducting polymers are rendered conductive through a conjugated bond system along the polymer backbone. They are typically formed either through chemical oxidation or electrochemical oxidation of the monomer. These conjugated polymers have an extended p-orbital system, through which electrons can move from one end of the polymer chain to the other. Conduction is achieved by inducing

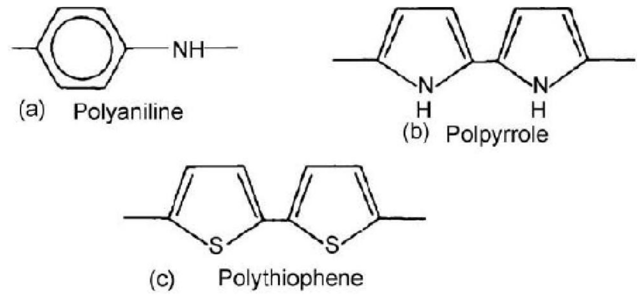

Figure 29 : Chemical structures of some conducting polymers[189]

a deficiency or excess of p-electrons in the polyconjugated chain, a process called doping by analogy with the insertion of electrons or holes in 3D inorganic semiconductors[185,186]. The electrical conductivity of these polymers is between 10^{-5} S/cm and 10^{2} S/cm while being doped, whereas common insulators exhibit conductivities below 10^{-12} S/cm. Conducting polymers are generally attractive as they have high charge density and low cost (compared with the relatively expensive metal oxides)[187,188]. Quite an extensive range of these polymers is now known and the maximum conductivity so far obtained is only a single order of magnitude below that of metallic copper[189].

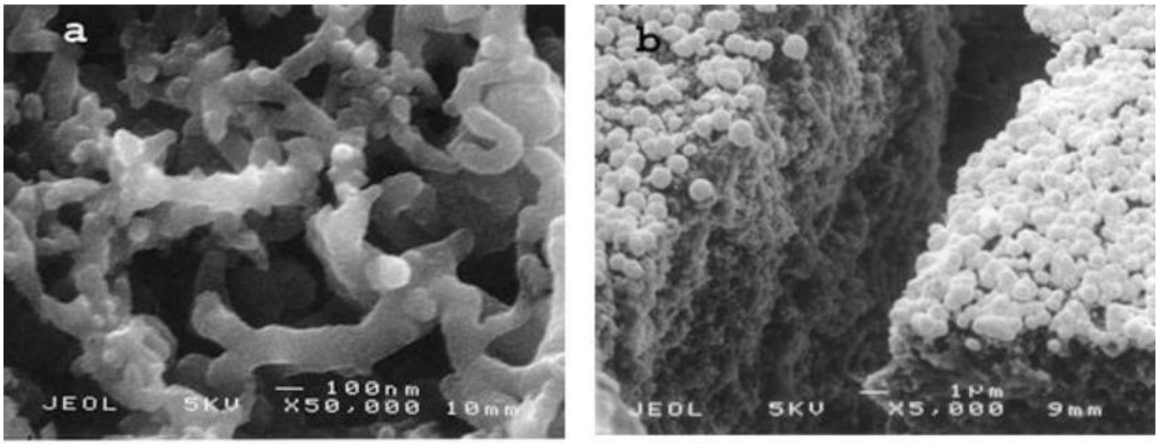

Figure 30 : (a) SEM of conventionally synthesized polyaniline. (b) SEM of the Pt particles on the conventionally synthesized polyaniline[202]

Metals conduct electricity through mobile electrons in the conduction band that travel across atoms in the lattice. The equivalent situation in organic materials is provided by delocalized p-electrons. Electrically conducting polymers have in common a significant overlap of delocalised p-electrons along the polymer chain, and several suitable structures are shown in Figure 29.

The physical and chemical properties (stability, conductivity, morphology, structure and catalytic activity) of various CP were carefully studied by many researches. Porous structure and high surface area of many conducting polymers promote their use as supporting material for the development of new catalytic and electrocatalytic materials. Because of a relative high electric conductivity of some polymers, it is possible to shuttle the electrons through polymer chains between the electrode and dispersed metal particles, where the electrocatalytic reaction occurs. Thus, an efficient electrocatalysis can be achieved at these composite materials, and a great deal of attention was paid to the use of conducting polymers as supporting matrices for the immobilization of catalytically active noble metal particles.

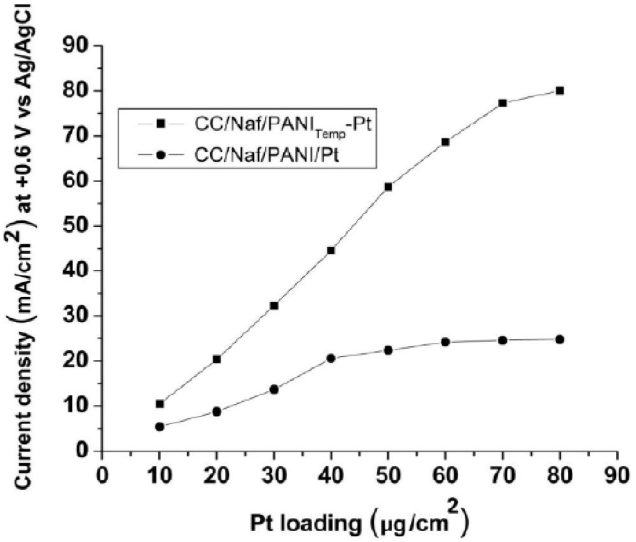

Figure 31 : Variation of electrocatalytic activity of methanol oxidation with Pt loading on nanotubule and conventional electrodes. ~Electrocatalytic activity were evaluated from CV run in 1 M H2SO4/1 M CH3 OH at 50 mV/s. The activity at 10.6 V *vs.* Ag/AgCl was taken for the measurement[202]

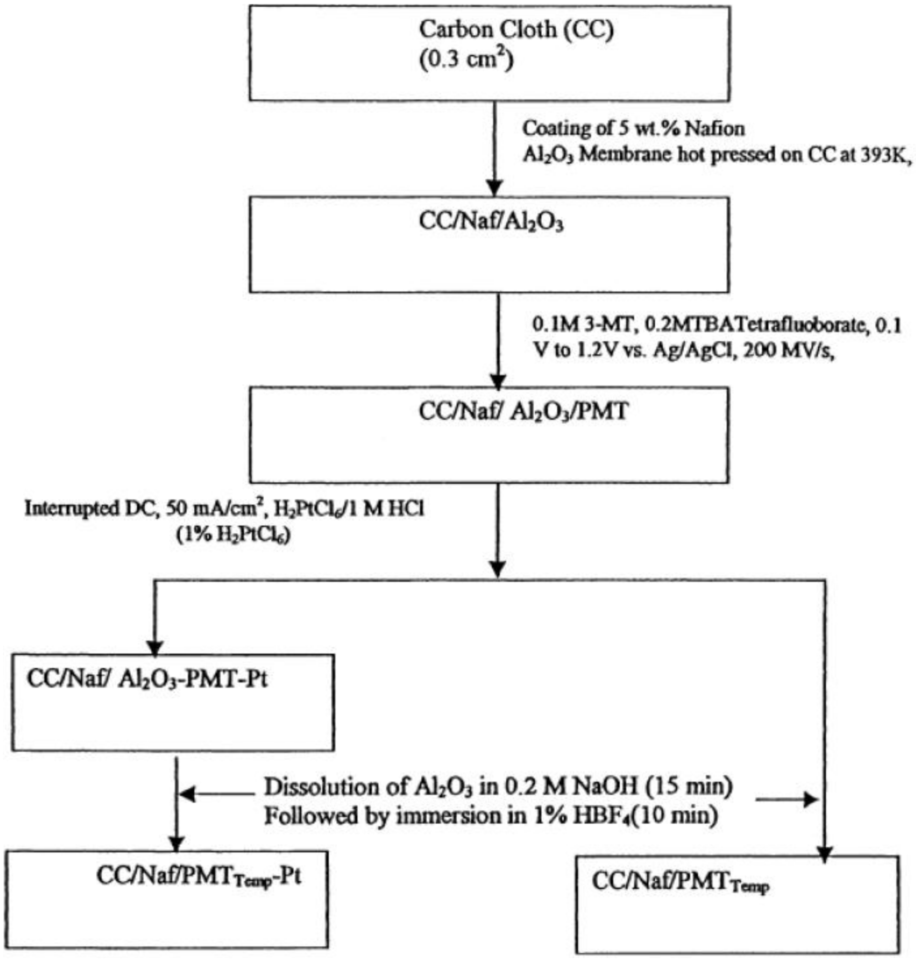

Figure 32 : Typical procedure for the template synthesis of poly(3-methyl) thiophene nanocones and Pt incorporated poly(3-methyl) thiophene nanocones[203]

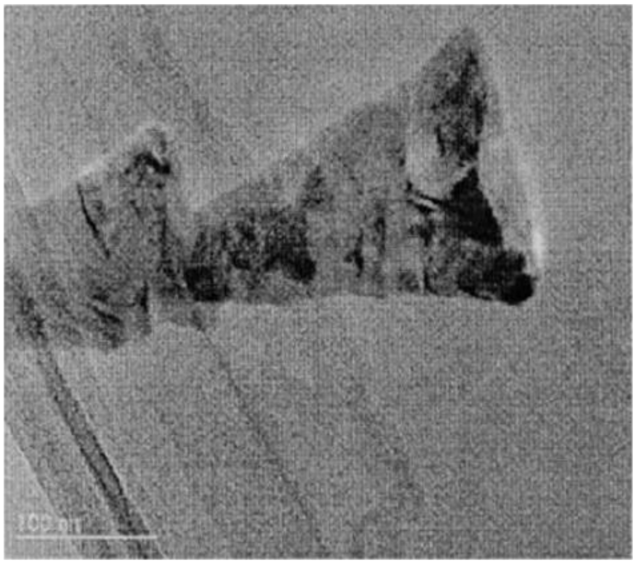

Figure 33 : HR-TEM image of poly(3-methyl) thiophene nanocones (withoutPt)[203]

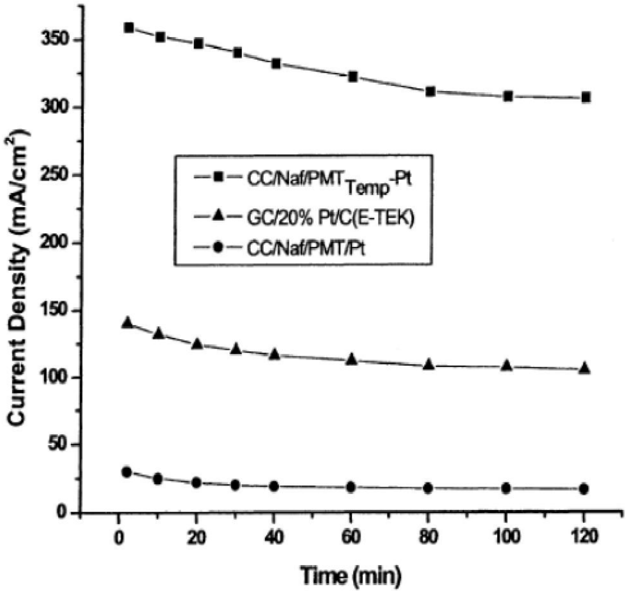

Figure 34 : Chronoamperometric response of CC/Naf/PMTTemp-Pt, GC/20 wt.%Pt/C (E-TEK) and CC/Naf/PMT-Pt electrodes in 1M H2SO4/1M CH3OH at +0.6V vs. Ag/AgCl[203]

The polymers that are most commonly studied for use as catalyst supports in fuel cell are polypyrrole

(PPy), polyaniline (PAni), polythiophene (PTh) and their derivatives (such as poly(3,4-ethylenedioxythiophene) (PEDOT).) Results of these studies were presented in numerous publications. Antolini, and Gonzalez[85] wrote a comprehensive review article about the, polymer supports for low-temperature fuel cell catalysts in 2009.

CPs can be synthesized in the form of one-dimensional nanostructures such as nanotubues, nanofibers, and nanowires are of particular interest, as their properties significantly differ from the properties of the corresponding macroscopic materials. Some of these special, physical, and chemical properties will render CPs useful for new applications in nanodevices[190].

It is acknowledged that typical nanomaterials or nanostructures have dimensions ranging from 1 to 100 nm. However, in the case of CPs this range is widened to about 500 nm. Many different techniques and strategies for formation of CP nanostructures have been developed and employed-ranging from template synthesis to no-template synthesis. For example recently the synthesis of nanotube[191], nanofibers[192,193], nanowires[194] and nanorods[195] morphology of polyanilin, nanowire array of Ppy[196-198] and nanorod[199] have been reported in literature. But as mentioned earlier because of the scope of this paper here we just report the results of nanostructure conductive polymers that used as support for low temperature fuel cell.

Deposition of Pt on conductive polymers based support

Metal particles can be included in the polymer matrix by electrodeposition or electroless precipitation. Electrodeposition of metals is the most widely used method to prepare metal/polymer composites. In general, there are two main approaches for electrodepositing metal particles in CP layers: (1) polymer electrosynthesis in the presence of metal precursors or preformed metal particles (one-step methods), and (2) polymer layer electro-synthesis (in the absence of metal) followed by metal electrodeposition (two-step methods). All the usual experimental techniques for producing metal deposits on inert conducting substrates, e.g., potentiostatic, galvanostatic, potentiodynamic, and also pulse techniques, have been applied for the second metal deposition step. It has to be promptly pointed out that, unlike carbon and ceramic materials, where the catalyst is localized on the support surface (two-dimensional array, 2D), in the case of polymer support,

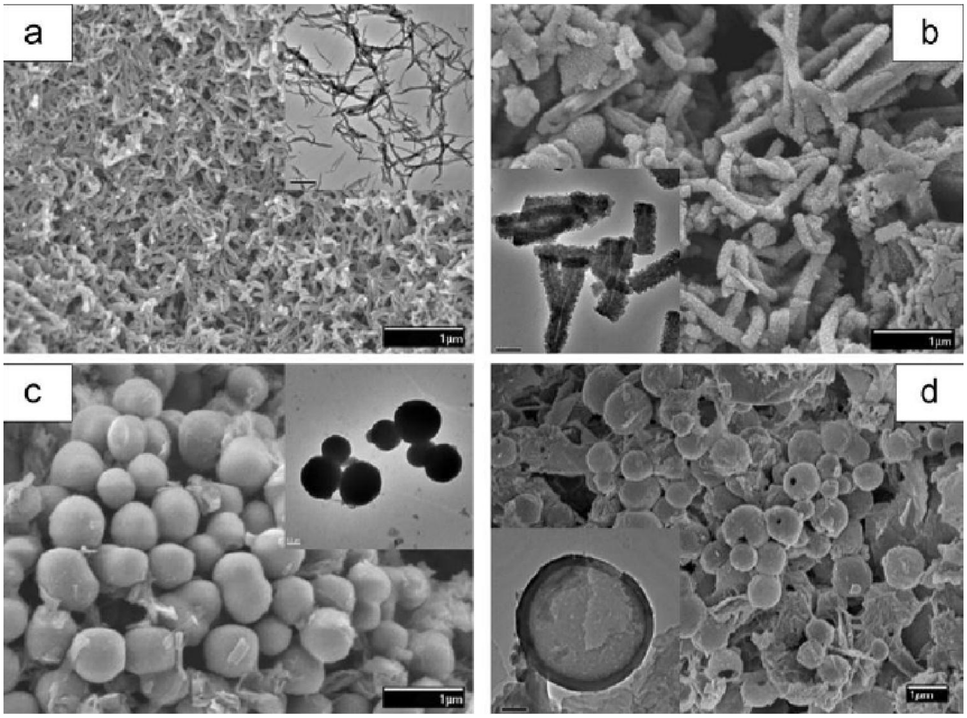

Figure 35 : SEM and TEM (corner) images of polyaniline micro/nanostructures: (a) nanofiber, (b) nanotubes, (c) submicron spheres, and (d) hollow microspheres. The reaction time for nanofibers and nanotubes is 90 min; the reaction time for submicron spheres and hollow microspheres is 45 min. The scale bar of the TEM image is 500 nm for nanofibers and 200nm for the others, respectively[204]

the catalyst can be also dispersed inside the matrix (three dimensional array, 3D), depending on the deposition method, catalyst loading and polymer thickness[82].

It was demonstrated that the tubular and fibrillar morphology of polymers plays an important role for the enhanced charge transport across the electrode/electrolyte interface and conductivity, compared to the conventionally synthesized polymers[200,201] On these bases, Rajesh et al.[202] investigated nanotubules of polyaniline as catalyst support for Pt nanoparticles for methanol oxidation by template method on commercial carbon cloth. In their investigation the electropolymerization was carried out on the template ~alumina membrane attached carbon cloth and, subsequently, Pt particles were electrodeposited before the dissolution of the template by NaOH. The electropolymerization was carried out by potentiodynamic method in 0.1M aniline and 1 M H_2SO_4. The potential was swept between 20.2 and 11.0 V at a scan rate of 50 mV/s. The resulting composite electrode was designated as CC/Naf/Al_2O_3 / PANITemp ~before the dissolution of alumina membrane. The platinum was electrodeposited by interrupted dc ~galvanostatic square wave method in 1% H_2PtCl_6 and 0.5 M H_2SO_4. The current density of 50 mA/cm^2 was applied for a total period of 2 to 8 min to vary the loading of Pt on the matrix. The pulse ~50 mA/cm^2 was applied initially for 10 s and stopped for 10 s until the total period was reached. The whole process of Pt deposition was done before the dissolution of the alumina membrane. The resulting configuration is designated as CC/Naf/Al_2O_3 /PANITemp-Pt. In order to remove the template the host ~alumina membrane from CC/Naf/Al_2O_3 /PANITemp and CC/Naf/Al_2O_3 / PANITemp-Pt was immersed in 0.1 M NaOH for 15 min. The preparation of conventional polyaniline and Pt deposited polyaniline was carried in the similar way as it has been done for the template synthesis method. In the conventional synthetic procedure, the polymerization and the subsequent Pt deposition on carbon cloth was done without the host alumina membrane. Figure 30a shows the SEM image of conventionally synthesized polyaniline on nafion coated carbon cloth. The image reveals the fibrillar and globular morphology of the conventionally synthesized polyaniline. The fibrils are randomly distributed without any orientation or alignment. Figure 30 b shows the SEM image of the Pt deposited on conventionally synthesized polyaniline. It is evident from the figure that large clusters of Pt particles of size around 100-150 nm are distributed throughout the polymer.In view of electrochemical activity the ohmic and the charge transfer resistances of the nanotube-based electrode were considerably lower than the polyaniline electrode synthesized by the conventional route. The Pt incorporated polyaniline nanotube electrode exhibited excellent catalytic activity and stability compared to the 20 wt % Pt supported on the VulcanXC 72R carbon and Pt supported on the conventional polyaniline electrode. Figure 31 shows the variation of performance of methanol oxidation current densities with Pt loading on CC/Naf/PANITemp-Pt and CC/Naf/ PANI/Pt electrodes.

In another study Rajesh and coworkers[203] reported the electrochemical synthesis of conducting nanocones of Pt incorporated poly(3-methyl) thiophene, employing alumina membrane templates and its use as an electrode material for methanol oxidation. The activity (131 mA/cm^2 at +0.4V versus Ag/AgCl for a Pt loading of 80 μg/cm^2) of nanocone-based electrode was found to be more than one order of magnitude higher compared to the regular poly(3-methyl) thiophene electrode (12.2 mA/cm^2 at +0.4V versus Ag/AgCl for a Pt loading of 80μg/cm^2). The chronoamperometric response confirms the better activity and stability of the nanocone-based electrode compared to the commercial 20 wt.% Pt/C (E-TEK) and template-free electrode. The XPS data confirmed the presence of Pt in the metallic state. According to the authors the nanocone morphology of poly (3-methyl) thiophene, helps in the effective dispersion of Pt particles facilitating the easier access of methanol to the catalytic sites. The details of the synthetic procedure for the preparation of template synthesized poly (3-methyl) thiophene and Pt incorporated template synthesized poly (3-methyl) thiophene are illustrated in Scheme 32.The HR-TEM image of poly (3-methyl) thiophene (without Pt) shown in Figure 33 clearly reveals the nanocone morphology of poly(3-methyl) thiophene with one cone inserted over the other cone.Fig. 34 shows the activity of CC/Naf/PMTTemp-Pt and CC/Naf/PMT-Pt with respect to time at +0.6V.The percentage decrease of the catalytic activity of CC/Naf/PMTTemp-Pt was around 14.3% at the end of 2 h (359–305.7 mA/cm^2), whereas the corresponding decrease for GC/20 wt.% Pt/C (E-TEK) was 25% (140–105 mA/cm^2) and for CC/Naf/PMT-Pt was 44.6% (30–16.6 mA/cm^2).The initial activity of CC/Naf/PMTTemp-Pt is higher by nearly 12 times compared to CC/Naf/PMT-Pt and 2.5 times compared to GC/20 wt.% Pt/C (E-TEK) electrodes. The Pt loading was kept at 80 μg/cm^2 for all the electrodes.

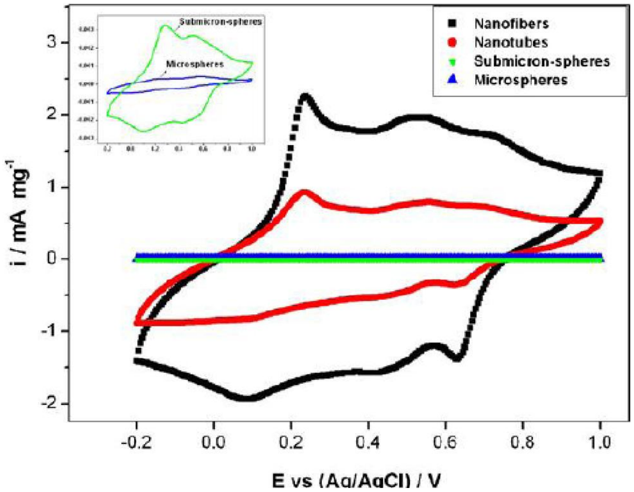

Figure 36 : Cyclic voltammogram curves of polyaniline micro/nanostructures in 1M CH3OH and 0.5M H2SO4 solutions[204]

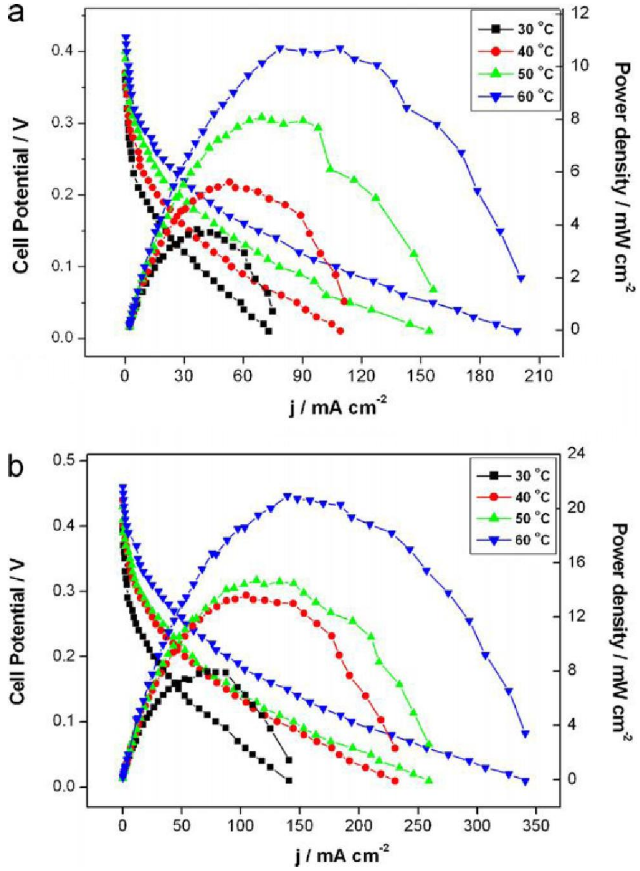

Figure 37 : Polarization curves of the DMFC using (a) XC-72 and (b) PANF supported Pt catalysts as anode. These catalysts were produced with the addition of 10mg PANF or XC-72 in the reaction solution[204]

Huang et.al[204] synthesized a series of micro/nanostructured polyanilines including submicron spheres, hollow microspheres, nanotubes, and nanofibers Figure 35 and investigated their morphology dependent electrochemical properties for acting as a catalyst supporter for direct methanol fuel cell (DMFC) applications.

Based on results in terms of electrochemical activity Figure 36 among the four micro/nanostructures, polyaniline nanofibers (PANF) manifest their superiority in high electrochemical active surface. Accordingly, PANF is adopted as the catalyst supporter. Compared with Pt/XC-72, the Pt/PANF electrode possesses higher electrocatalytic activity and exhibits double power density Figure 37.

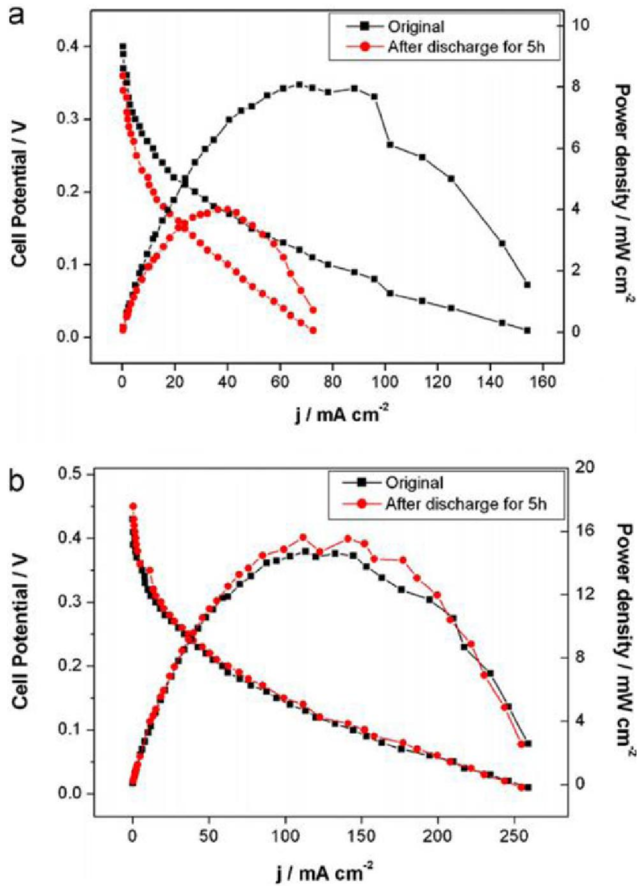

Figure 38 : Polarization curves of the DMFC using (a) XC-72 and (b) PANF supported Pt catalysts as anode after a continuous discharge at 0.3V and 50 °C for 5 h. These catalysts were produced by adding 10mg of PANF or XC-72 in the reaction solution[204]

Moreover, Pt/PANF is superior to Pt/XC-72 in the aspect of operation stability based on a continuous discharge for 5 h Figure 38.

Furthermore more recently Zhiani et.al[205] fabricated a novel nanostructure membrane-electrode assembly (MEA) prepared by employing of the polyaniline (PANI) modified anode for DMFC and characterized by SEM and polarization curves in DMFC under different conditions. Figure 39 a and b demonstrates the formation of PANI nanofibers within the anode catalyst layer and confirms the PANI nanofibers formation within the electrode.

The DMFC test results under steady state conditions indicated that the novel nanostructure MEA exhibited higher performance compared to the conventional MEA in term of maximum power density and resistivity against methanol crossover from the anode side to the cathode side. Maximum power density of 105 mW /cm^2 was obtained by new PANI modified anode compared to 75 mW /cm^2 by conventional anode in the same conditions Figure 40. They attributed the enhanced performance to the higher activity of the PANI modified anode and lower methanol crossover caused by the PANI as barrier in the modified anode.

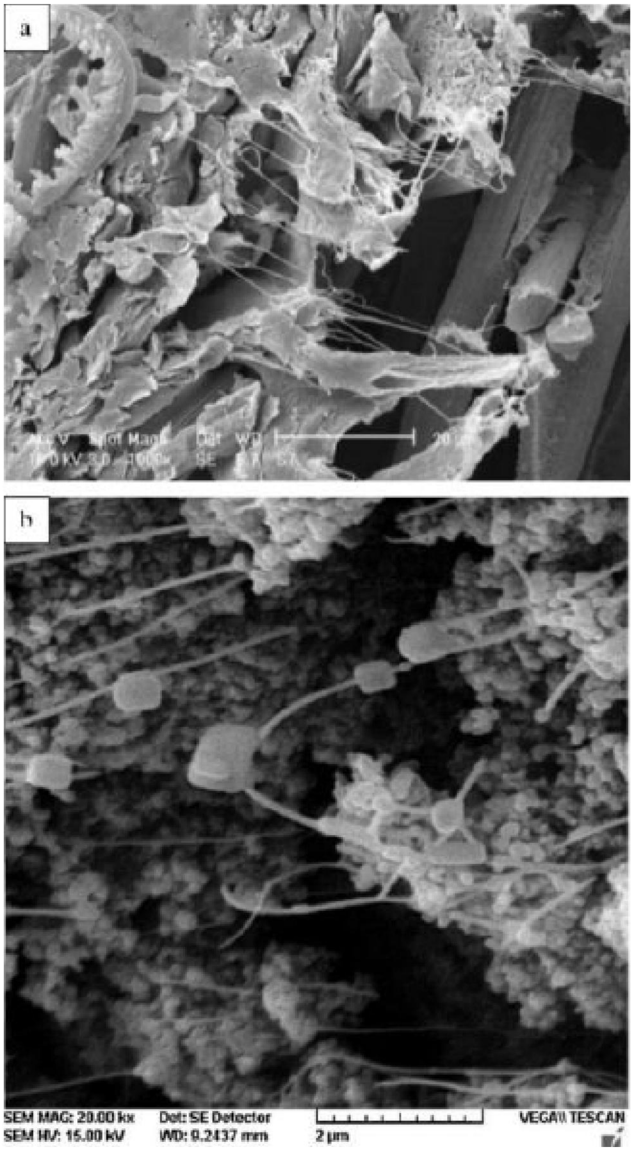

Figure 39 : Top view of scanning electron microscopy (SEM) image of the PANI modified anode (a). SEM image of the PANI modified catalyst layer (b)[205]

Composite nanostructure material -supported Pt nanoparticles: Characterization and electrochemical activity performance as anode and cathode

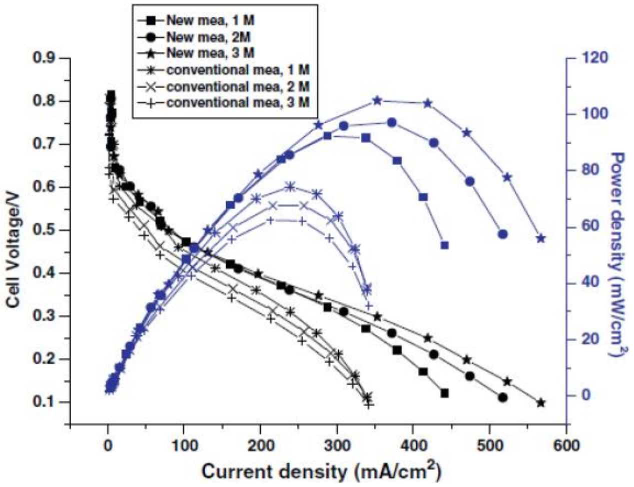

Figure 40 : Performance of the novel MEA and conventional MEA at 80°C and different methanol concentrations: 1, 2 and 3 M, PO2 : ambient, O2 flow rate: 0.2 ml/ min, anode and cathode catalyst loading: 4 and 2 mg/ cm2, respectively[205]

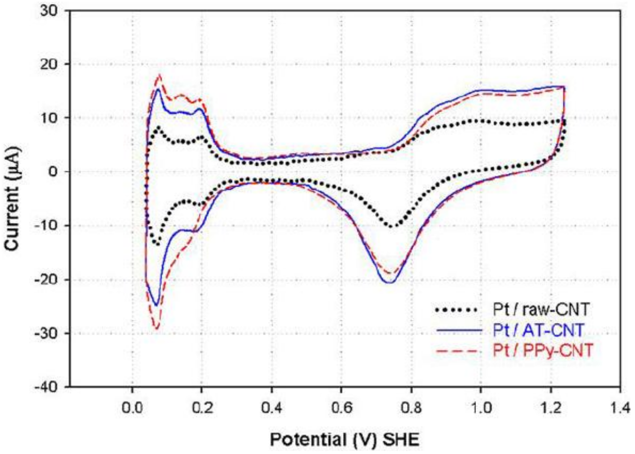

Figure 41 : Comparison of Cyclic voltammograms using the Pt/raw CNTs, Pt/AT-CNTs(acid-treated CNTs) and Pt/PPy-CNTs(PPycoated CNTs) in 0.5 M H2SO4[218]

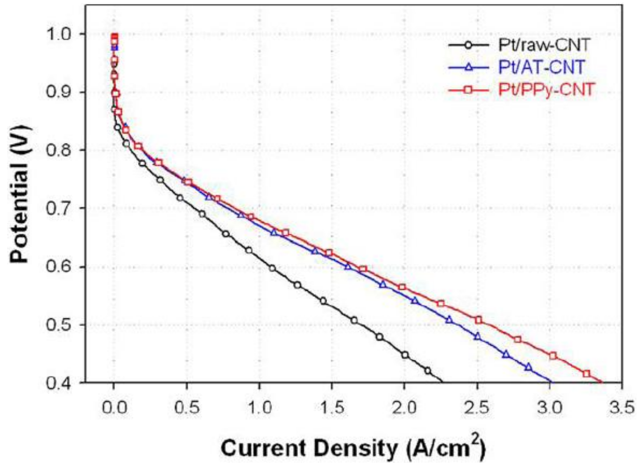

Figure 42 : Comparison of MEA performance using the Pt/raw CNTs, Pt/AT-CNTs and Pt/PPy-CNTs[218]

catalysts for PEM fuel cell

Summarizing, the use of either carbon or ceramic or polymer materials as fuel cell catalyst support is not absolutely satisfactory. Thus, in the last years composite polymer–carbon, ceramic–carbon and polymer–ceramic materials have been proposed as fuel cell catalyst supports. These composite materials can possess more suitable properties for their use as catalyst supports than their individual components. It was shown that the combination of PAni with CNTs would offer an attractive composite support material for electrocatalyst to enhance its activity and stability based on morphological modification and/or electronic interaction between two components. The results of these works have been congregated by Antolini's review papers[206].

Among the hybrid of conducting polymers and CNTs, the composites of PAni -CNT and Ppy-CNT are the most investigated hybrid supports for fuel cell catalyst and numerous papers have been reported the improved of electrode properties by use of these materials as a support by different authors[207-218] They ascribed these improvements to the enhance the thermal, mechanical, electrical and high available surface area (the high catalyst dispersion to the charge from hydrophobic surface of pristine CNTs to more hydrophilic polymer coated-CNTs surface) and easier charge transfer at polymer/electrolyte interface allowing a high utilization of deposited metal nanoparticles. These polymers-CNT supported catalyst showed high activity for methanol, formic acid oxidation and oxygen reduction reaction as well. For example Oh and coworkers[218] prepared Polypyrrole-modified hydrophobic carbon nanotubes as promising electrocatalyst supports in polymer electrolyte membrane fuel cells. In their study, however, the modified polyol process was used to deposit Pt nanoparticles on PPy-coated CNTs without lowering the Pt utilization. In addition, the thickness of the PPy coating was precisely controlled and its effects on the performance of fuel cells and the sintering of Pt nanoparticles were explored. As an alternative to oxidative acid treatment, a hydrophobic graphitized carbon nanotube (CNT) was functionalized with 1-4 nm thick polypyrrole (PPy) prior to application as catalyst supports in polymer electrolyte membrane (PEM) fuel cells. Unlike oxidative acid treatment, the PPy coating method converts the hydrophobic surface of a CNT to a hydrophilic one without creating defects on the surface of the CNT. As a result, Pt nanoparticles deposited on the PPy-coated CNTs showed an improved distribution, which significantly enhanced the fuel cell performance while preserving the intrinsic properties of the CNTs, i.e., resistance to electrochemical carbon corrosion. The ESA of the Pt/raw CNTs, as determined by a CV experiment in Figure 41, was calculated to be 39.4 m^2/ g, which is lower than the others because of the poor distribution of Pt nanoparticles. The ESA of the Pt/AT-CNTs was 56.7 m^2 /g, and it was further increased to a value of 65.1 m^2/ g when the Pt nanoparticles were deposited on the PPy-CNTs.Figure 42 shows the performance of PEM fuel cells prepared with the different cathode catalysts, Pt/raw-CNFs, Pt/AT-CNTs and Pt/PPy-CNTs. The cathode catalyst loadings were maintained at 0.4 mg /cm^2. At a cell potential of 0.6 V, the current density of the Pt/PPy-CNTs was 1.71 A /cm^2, which is higher than that of the Pt/AT-CNTs (1.61 A /cm^2) and significantly enhanced in comparison to that of the Pt/raw CNTs (1.09 A/ cm^2). This attributed to the improved distribution of Pt nanoparticles and high ESA for the Pt/PPy-CNTs.

The preparation of carbon–ceramic nanostructure materials has generated a great deal of interest since they demonstrate properties that cannot be attained by their individual components. As an example, the formation of nanocomposites with carbon and ceramic nanomaterials has been found to enhance the mass activity and chemical properties of the latter. In the experiments that conducted by Bauer and coworkers[219] platinum catalyst nanoparticles (20 wt.%) were deposited on a mixed support, which consisted of 25 at.% Nb doped TiO_2 nanofibers and carbon agglomerates Figure 43.

The catalyst was characterized electrochemically with respect to durability and oxygen reduction activity. Based on cyclic voltammetry tests Figure 44, the Nb–TiO_2/C supported catalyst was more stable compared to a commercially available carbon supported Pt catalyst (E-tek) over 1000 cycles. The apparent active Pt area decreased by 5% due to cycling, whereas in the case of Pt/C the decrease was 23%. The oxygen reduction performance was comparable for both cases. For example, during the anodic sweep the mass activity at 0.9 V vs. the reversible hydrogen electrode (RHE) was 19 A /gPt and 20 A /gPt for the freshly prepared in-house prepared and commercial catalysts, respectively. After the durability experiment both types of catalysts yielded a mass activity of 17 A /gPt. They also examined fuel cell tests with a single cell configuration with the Nb–TiO_2/C supported catalyst on the cathode side (gas diffusion electrode). The measurements were yielded a peak power density of 0.34 W /cm^2 at 75 °C when pure oxygen was supplied on the cathode side Figure 45.

Hu and coworkers[220] have prepared Pd nanoparticles on tungsten carbides modified multiwalled carbon nanotubes (Pd-WC/MWCNT) catalysts by an intermittent microwave heating (IMH) technique. The Pd-WC/MWCNT catalysts were evaluated and showed an improved kinetics for the ethanol oxidation. It is recognized that the significant increase in the catalytic activity for ethanol oxidation on Pd-WC/MWCNT is attributed to both the synergistic effect between Pd nanoparticles and the WC support and the structure effect of the MWCNT. They proposed this type catalyst can be universally used as the oxygen reduction catalyst in fuel cells and sensors both in alkaline and acidic solutions.

Metal oxide coated carbon nanotube (CNT) was successfully used as a support for fuel cell catalyst. On this basis Du and coworkers[221] prepared a novel CNT@SnO_2 nanocomposite (in which the inner layer was comprised of CNT and the outer layer was SnO_2, forming a core-shell structure) as a stabilizing support for catalysts of proton exchange membrane fuel cells. Figure 46 presents a TEM image of the CNT@SnO_2 nanocomposite for catalyst support material of PEMFCs. Clearly, uniform dark SnO_2 sheath could be observed on the surface of the CNT core, reflecting that the CNT had been completely coated by a SnO_2 layer. The CNT@SnO_2 composite showed a much lower anodic current than the CNT Figure 47, especially at high potentials, representing the CNT@SnO_2 was more corrosion resistant.

The Pt/(CNT@SnO_2) catalyst was electrochemically active and exhibited comparable activity for the oxygen reduction reaction to the CNT supported catalyst (Pt/CNT). More importantly, the long-term stability of the Pt/(CNT@SnO_2) catalyst was significantly higher than that of the Pt/CNT catalyst, which might be mainly due to the fact that the CNT@SnO_2 was more corrosion resistant and mesoporous SnO_2 was beneficial to restrict the Pt migration and aggregation (Figure

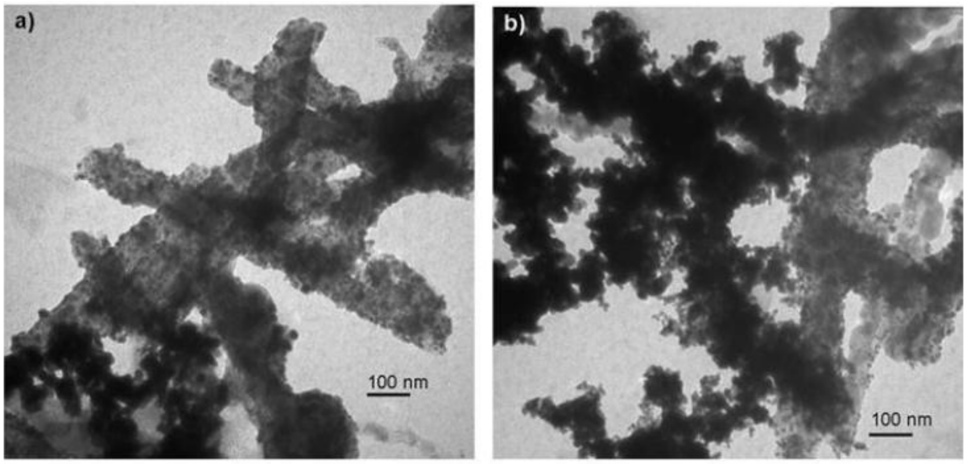

Figure 43 : TEM micrographs of Pt dispersed on the mixed Nb doped TiO2 nanofiber–carbon substrate. The micrographs show examples of regimes with relatively low (a) and higher (b) carbon content, respectively[219]

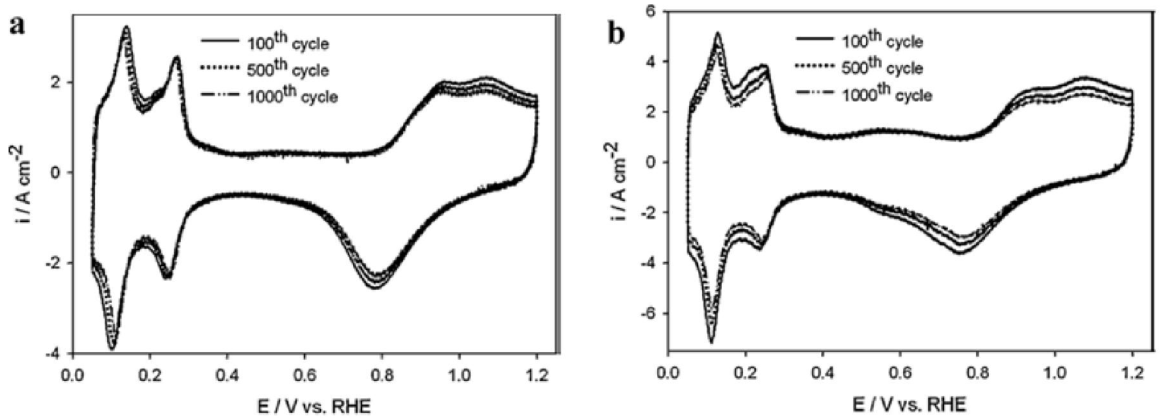

Figure 44 : Voltammetric stability experiment conducted with Pt supported on the Nb–TiO2 nanofiber–carbon composite (a) and Pt supported on commercially avail-able carbon (E-Tek) (b). Conditions: 0.5 M H2SO4 (N2 purged), potential scan rate = 100 mV/ s[219]

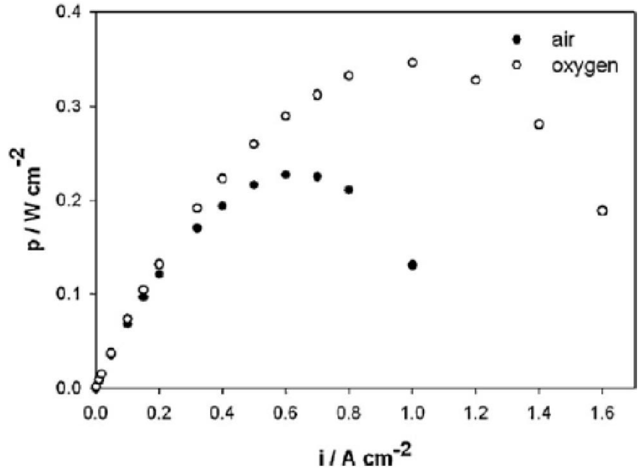

Figure 45 : Fuel cell polarization tests. Conditions: 100% relative humidity, 75 °C, oxidant flow rate = 1 l/ min, hydrogen flow rate = 0.5 l /min, no backpressure applied[219]

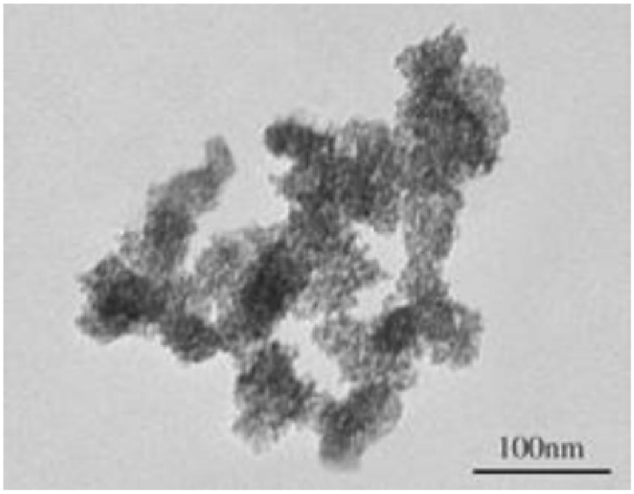

Figure 46 : TEM image of the CNT@SnO2 core–sheath nanocomposite prepared by the hydrothermal method[221]

48). Based on these results they concluded that the CNT@SnO$_2$ would be a promising durable catalyst

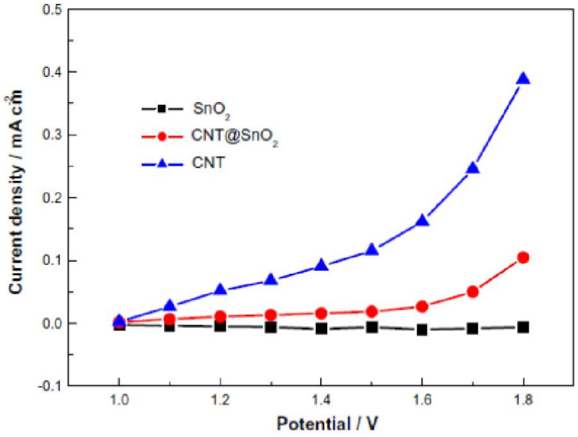

Figure 47 : Steady-state corrosion currents of the CNT@SnO2, SnO2 and CNT in N2-purged 0.5 M H2SO4 solution as a function of polarization potential[221]

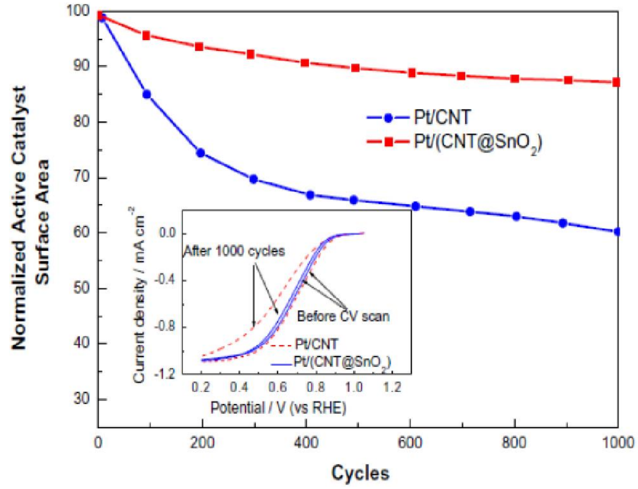

Figure 48 : Normalized active catalyst surface areas of the Pt/(CNT@SnO2) and Pt/CNT catalysts versus the cumulative number of potential cycles in N2-purged 0.5 M H2SO4 solution. Inset: Polarization curves of the Pt/(CNT@SnO2) and Pt/CNT catalysts in 0.5 M H2SO4 solution saturated with O2 using a rotating disk electrode at 2500 rpm[221]

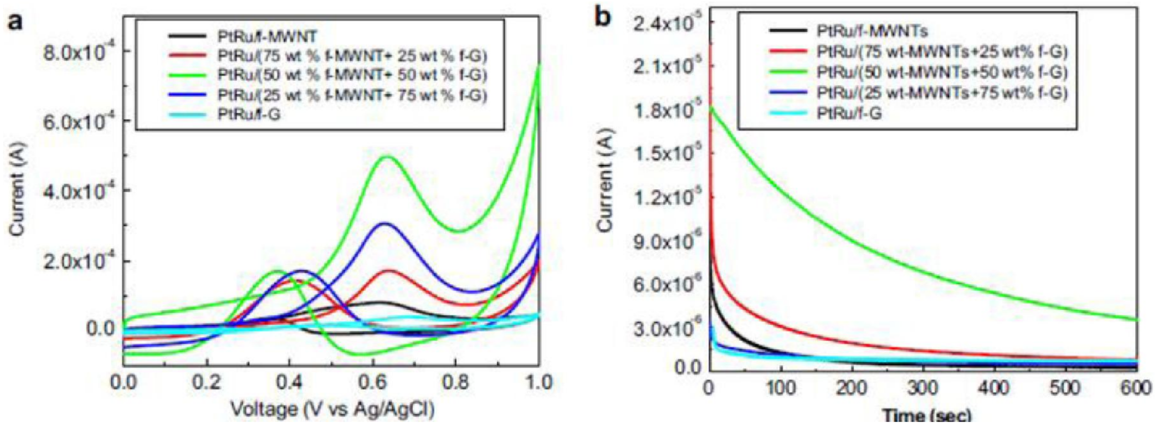

Figure 49 : (a) CV of anodic electrocatalyst in 1 M methanol + 1 M H2SO4, Scan rate was 50 mV/s (b) Chronoamperometry curve of anodic electrocatalyst in 1 M methanol + 1 M H2SO4[222]

support for PEMFCs.

Regarding the Graphene-CNT hybrid electrocatalyst support material Jha et.al[222] prepared Nanostructured PtRu and Pt dispersed functionalized graphene -functionalized multi walled carbon nanotubes (PtRu/(f-Gef-MWNT)), (Pt/(f-Gef-MWNT)) nanocomposites. Electrochemical studies have been performed for the methanol oxidation using cyclic voltammetry (CV) and chronoamperometry technique. Fuel cell measurements have been performed using PtRu nanoparticles dispersed on the mixture of functionalized graphene (f-G) and functionalized multi walled carbon nanotubes (f-MWNT) in different ratios as anode electrocatalyst for methanol oxidation and Pt/f-MWNT as cathode catalyst for oxygen reduction reaction in direct methanol fuel cell (DMFC). Figure 49 a shows CV of electrocatalysts after 50 cycles of activation indicating two methanol oxidation peaks, corresponding to oxidation of methanol in forward scan and its intermediates in reverse scan. Value of peak current and area under the CV curves are proportional to methanol oxidation activity of the electrocatalyst. Ratio of forward anodic peak current (If) to reverse anodic peak current (Ib) shows the tolerance ability of electrocatalysts to accumulation of carbonaceous products. Chronoamperometry has been performed to measure catalytic stability of the electrocatalysts Figure 49 b. The current measured for PtRu/ (50 wt% f-MWNT +50 wt% f-G) is much higher compared to other electrocatalysts during the whole testing time indicating higher stability of the catalyst. Hence one can conclude that the hybrid material with f-MWNT and f-G in equal ratio is the best alternative for anode catalyst support.

CONCLUSION

Fuel cells have been known for a long time and still are under development. Several challenges to widespread implementation of PEM fuel cell technology are needed, although novel inexpensive and long-term electrocatalysts materials are key factors in design and development. In all fuel cells including low temperature fuel cells the overpotential for the reduction of oxygen at operating currents is significantly high due to the slow oxygen electrochemical kinetics. As a result of this sluggish kinetics, cell voltage is decreased and therefore fuel cells loss in efficiency. Therefore the high overpotential for oxygen reduction is a foremost problem and, so far, research on the fundamental process of oxygen reduction and catalysis has not yielded a breakthrough by the current fuel cell cathode catalyst. Thus, new alternatives for finding materials with lower overpotential are needed. Recent advances in application of nanostructured carbonaceous-based and also non carbonaceous-based materials have suggested the possibility of using these materials as novel electrocatalysts supports. Studies have shown that Pt nanoparticles supported on nanostructured carbonaceous-based and also non carbonaceous-based materials display remarkably higher electrocatalytic activity toward the reduction of oxygen than Pt nanoparticles supported on carbon black, which would contribute to substantial cost reduction in PEM fuel cells. The finite size of nanoscale materials positively influences the thermodynamics and kinetics of oxygen reduction due to their length scale and specific properties. In general, their unique characteristics encourage the use of nanosize electrocatalysts materials instead of their bulk counterparts to enhance the oxygen electroreduction performance.

This article reviewed various non-carbonaceous nanostructured based materials as a catalyst support including metal oxides and carbides nanowires (NWs), nanorods, the nanostructer of conductive polymers e.g. PAni / PPy nanofibers, and PAni / PPy nanowires as well as composites of these nanostructured catalyst support materials as substitute of carbon black to improve the performance and durability of electrodes through increasing electrocatalytic activity and Pt utilization.Various preparation methods for active electrocatalyst have been examined with some consideration from practical points of view associated with each preparation method. Types of catalyst supports and their structure (also.properties) along with some synthetic strategies for selected support types have been also explored based on the recent literature for low temperature fuel cell application. It was started by introducing NWs and nanostructure CPs with unique structures and excellent mechanical, thermal and electric properties which have been explored as novel catalyst supports for PEM fuel cell catalyst. For the synthesis of NWs and nanostructure CPs supported Pt catalyst several synthesis methods were discussed. These studies have reveled that the morphology and catalytic activity of Pt/NWs and Pt/CPs catalyst are seriously affected by their corresponding synthesis methods. These were all closely related to the utilization and performance of the catalysts in fuel cells . We also discussed about the durability issues of PEM fuel cell by using NWs and nanostructure CPs based electrode which have been considered of the major barriers to the commercialization of fuel cell. Metal oxides (eig. tungusten oxides) and metal (e.g Pt nanowires) based nanostructure also investigated and have shown interesting results and have strong potential for further development. It was reported that the nanowire-based electrode exhibited higher electrocatalytic activity both for the oxygen reduction reaction and the methanol oxidation reaction as well as enhanced the CO tolerance in comparison to a standard Pt/C electrode[223]. Therefore, it is expected that integrated three dimensional nanowire-based fuel cell electrodes will be ideal materials for providing a higher catalytic performance, higher catalyst utilization, efficient mass transport, and a longer fuel cell operational life. The use of nanostructured morphology of CPs like PAni and PPy NFs and NWs recently have received great interest. Nanostructure of CPs regardless their extraordinary properties thanking of their morphologies considering their capabilities of proton and electron conductivity, water and gas permeability, these sorts of supports may be considered as ideal supports in the near future. It is hypothesized that the electrodes that are made using CP nanostructure catalyst would need less nafion in the catalyst layer. Interest in nanothechnology has greatly stimulated research on carbonaceous materials, such as CNTs/CNFs and graphene NPs. Development of nanostructures afforded by ceramic and CP proceeds independently and includes the nanotubes, nanofibers and nanowires as well as coating of various substrates with a thin polymer film. The combination of both types of materials on a nanosize level is thus an obvious challenge. So the use of hybrid supports can bring the best of both carbonaceous supports. These approaches are illustrated by the coating of CNT with CP and CNT-ceramic materials system in this review.

In conclusion nanotechnology is evident in the recent developments for PEM fuel cells. Whilst much is reported on the preparation of highly dispersed Pt and Pt-alloy catalyst, it is recognized that improvements can be made to the nanostructured electrocatalysts support. In this context non-carbonaceous nanostructured based materials, e.g metal oxides and carbides nanowires (NWs), nanorods, the nanostructer of conductive polymers e.g. PAni / PPy nanofibers, and PAni / PPy nanowires as well as composites of these nanostructured catalyst support materials proved to be better alternatives than the high surface area and conductive carbon black.

REFERENCES

[1] P.Raveendran,J.Fu, S.L.Wallen; J.Am.Chem.Soc., **125**, 13940 **(2003)**.

[2] J.A.Dahl,B.L.S.Maddux, J.E.Hutchison; Chem.Rev.Columbus, **107**, 2228 **(2007)**.

[3] L.Zhang, J.Zhang, D.P.Wilkinson, H.Wang; J.Power Sources, **156**, 171 **(2006)**.

[4] H.Liu, C.Song, L.Zhang, J.Zhang, H.Wang, D.P.Wilkinson; J.Power Sources, **155**, 95 **(2006)**.

[5] K.Lee, J.Zhang, H.Wang, D.P.Wilkinson; J.Appl.Electrochem, **36**, 507 **(2006)**.

[6] R.Bashyam, P.Zelenay; Nature, **443**, 63 **(2006)**.

[7] A.Guha, W.Lu, T.A.Zawodzinski Jr., D.A.Schiraldi; Carbon, **45**, 1506 **(2007)**.

[8] P.Costamagna, S.Srinivasan; J.Power.Sources, **102**, 253 **(2001)**.

[9] A.Faur; Ghenciu Curr Opin Solid State Mater.Sci., **6**, 389 **(2002)**.

[10] V.Mehta, J.S.Cooper; J.Power Sources, **114**, 32 **(2003)**.

[11] H.A.Gasteiger,S.S.Kocha, B.Sompalli, F.T.Wagner; Applied Catalysis B: Environmental, **56**, 9 **(2005)**.

[12] P.J.Bouwman, W.Dmowski, J.Stanley, G.B.Cotten, K.E.Swider-Lyons; Journal of the Electrochemical Society, **151**, A1989 **(2004)**.

[13] M.Shao,T.Huang, P.Liu, J.Zhang, K.Sasaki, M.Vukmirovic, R.Adzic; Langmuir, **22**, 10409 **(2006)**.

[14] O.Savadogo, K.Lee, K.Oishi, S.Mitsushima, N.Kamiya, K.I.Ota; Electrochem Commun **6**, 105 **(2004)**.

[15] M.H.Shao, K.Sasaki, R.R.Adzic; J.Am.Chem.Soc., **128**, 3526 **(2006)**.

[16] V.Raghuveer, P.Ferreira, A.Manthiram; Electrochem Commun, **8**, 807 **(2006)**.

[17] V.Raghuveer, A.Manthiram, A.J.Bard; J.Phys.Chem.B, **109**, 22909 **(2005)**.

[18] M.Shao, P.Liu, J.Zhang, R.Adzic; J.Phys.Chem.B., **111**, 6772 **(2007).**

[19] A.Bouwkamp-Wijnoltz, W.Visscher, J.Van Veen, S.Tang; Electrochim Acta, **45**, 379 **(1999)**.

[20] J.H.Wee, K.Y.Lee, S.H.Kim; J.Power Sources, **165**, 667 **(2007)**.

[21] R.O'Hayre, S.J.Lee, S.W.Cha, F.B.Prinz; J.Power Sources, **109**, 483 **(2002)**.

[22] D.Gruber, N.Ponath, J.Muller, F.Lindstaedt; J.Power Sources, **150**, 67 **(2005)**.

[23] M.S.Saha, A.F.Gullb, R.J.Allen, S.Mukerjee; Electrochim Acta, **51**, 4680 **(2006)**.

[24] J.Lee, J.Seo, K.Han, H.Kim; J.Power Sources, **163**, 349 **(2006)**.

[25] N.Cunningham, E.Irissou, M.Lefevre, M.C.Denis, D.Guay, J.P.Dodelet; Electrochem Solid-State.Lett., 6, A125 **(2003)**.

[26] S.Cha, W.Lee; Journal of the Electrochemical Society, **146**, 4055 **(1999)**.

[27] Y.H.Cho, S.J.Yoo, H.S.Park, I.S.Park, J.K.Lee, Y.E.Sung; Electrochim Acta, **53**, 6111 **(2008)**.

[28] D.Gruber, J.Muller; J.Power Sources, **171**, 294 **(2007)**.

[29] R.Maric, J.M.Roller, R.Neagu, K.Fatih, A.Tuck; Low Pt thin cathode layer catalyst layer by reactive spray deposition technology. Fuel cell seminar & exposition, (ECS Transactions 2008), **(2008)**.

[30] S.Hirano, J.Kim, S.Srinivasan; Electrochim Acta, **42**, 1587 **(1997)**.

[31] A.T.Haug, R.E.White, J.W.Weidner, W.Huang, S.Shi, T.Stoner, N.Rana; J.Electrochem Soc., **149**, A280 **(2002)**.

[32] A.Caillard, P.Brault, J.Mathias, C.Charles, R.Boswell, T.Sauvage; Surf Coat Technol, **200**, 391 **(2005)**.

[33] P.Brault, A.Caillard, A.Thomann, J.Mathias, C.Charles, R.Boswell, S.Escribano, J.Durand, T.Sauvage; J.Phys.D: Appl.Phys., **37**, 3419 **(2004)**.

[34] A.J.J.Kadjo, P.Brault, A.Caillard, C.Coutanceau, J.P.Garnier, S.Martemianov; J.Power Sources, **172**, 613 **(2007)**.

[35] S.Charojrochkul, K.Choy, B.Steele; J.Eur.Ceram.Soc., **24**, 2515 **(2004)**.

[36] S.Charojrochkul, R.Lothian, K.Choy, B.Steele; J.Eur.Ceram.Soc., **24**, 2527 **(2004)**.

[37] R.Breitkopf, F.Maniei, A.Hunt, J.Hwang; Carbon supported Pt nanomaterials for fuel cell applications using combustion chemical vapor condensation. pp. 4902003).

[38] H.Song, C.Xia, G.Meng, D.Peng; Thin Solid Films, **434**, 244 **(2003)**.

[39] Y.Liu, M.Liu; Nano-Particles and Nanostructured Electrodes Fabricated by Combustion CVD. (The Electrochemical Society, 2003) 205 **(2003)**.

[40] R.Maric; Reactive spray formation of coatings and powders. (WO Patent WO/2007/045,089, 2007), **(2007)** .

[41] Y.Liu; Georgia Institute of Technology, Georgia Tech Theses and Dissertations, **(2005)**.

[42] A.Hunt, W.Carter, J.Cochran; Applied physics letters, **63**, 266 **(1993)**.

[43] E.Gulzow, M.Schulze, N.Wagner, T.Kaz, R.Reissner, G.Steinhilber, A.Schneider; J.Power

Sources, **86**, 352 **(2000)**.

[44] E.Giilzow, M.Schulze, N.Wagner, T.Kaz, A.Schneider, R.Reissner; Fuel Cells Bulletin, **2**, 8 **(1999)**.

[45] R.Benitez, J.Soler, L.Daza; J.Power Sources, **151**, 108 **(2005)**.

[46] A.Chaparro, R.Benitez, L.Gubler, G.Scherer, L.Daza; J.Power Sources, **169**, 77 **(2007)**.

[47] H.Morikawa, N.Tsuihiji, T.Mitsui, K.Kanamura; J.Electrochem Soc., **151**, A1733 **(2004)**.

[48] R.Louh, H.Huang, F.Tsai; Journal of fuel cell science and technology, **4**, 72 **(2007)**.

[49] R.F.Louh, A.C.C.Chang, V.Chen, D.Wong; Int.J.Hydrogen Energy, **33**, 5199 **(2008)**.

[50] T.Nakakubo, M.Shibata, K.Yasuda; J.Electrochem Soc., **152**, A2316 **(2005)**.

[51] C.H.Wan, M.T.Lin, Q.H.Zhuang, C.H.Lin; Surf Coat Technol, **201**, 214 **(2006)**.

[52] J.Zhang; PEM fuel cell electrocatalysts and catalyst layers: fundamentals and applications. (Springer Verlag). **(2008)**

[53] M.K.Debe, A.K.Schmoeckel, G.D.Vernstrom, R.Atanasoski; J.Power Sources, **161**, 1002 **(2006)**.

[54] Z.Liu, X.Lin, J.Y.Lee, W.Zhang, M.Han, L.M.Gan; Langmuir, **18**, 4054 **(2002)**.

[55] R.Yu, L.Chen, Q.Liu, J.Lin, K.L.Tan, S.C.Ng, H.S.O.Chan, G.Q.Xu, T.S.A.Hor; Chem.Mater, **10**, 718 **(1998)**.

[56] E.S.Steigerwalt, G.A.Deluga, C.Lukehart; J.Phys.Chem.B, **106**, 760 **(2002)**.

[57] T.Hyeon, S.Han, Y.E.Sung, K.W.Park, Y.W.Kim; Angewandte Chemie, **115**, 4488 **(2003)**.

[58] N.Rajalakshmi, N.Lakshmi, K.Dhathathreyan; Int.J.Hydrogen.Energy, **33**, 7521 **(2008)**.

[59] X.Cui, J.Shi, H.Chen, L.Zhang, L.Guo, J.Gao, J.Li; J.Phys Chem B **112**, 12024 **(2008)**.

[60] H.Zhao, L.Li, J.Yang, Y.Zhang, H.Li; Electrochem Commun, **10**, 876 **(2008)**.

[61] E.Antolini, E.Gonzalez; Solid State Ionics, **180**, 746 **(2009)**.

[62] E.Antolini; Appl.Catal, B :Environmental, **88**, 1 **(2009)**.

[63] A.WiÄ™ckowski, E.R.Savinova; Catalysis and electrocatalysis at nanoparticle surfaces. (CRC Press). **(2003)**

[64] M.Pourbaix, M.Pourbaix; Published 1974 by NACE, 644 **(1974)**.

[65] J.Liu, Z.Zhou, X.Zhao, Q.Xin, G.Sun, B.Yi; Phys.Chem.Chem.Phys., **6**, 134 **(2004)**.

[66] Y.Shao, G.Yin, J.Zhang, Y.Gao; Electrochimica acta, **51**, 5853 **(2006)**.

[67] Y.Shao, G.Yin, Z.Wang, Y.Gao; Journal of Power Sources, **167**, 235 **(2007)**.

[68] E.S.Steigerwalt, G.A.Deluga, D.E.Cliffel, C.Lukehart; J.Phys.Chem.B, **105**, 8097 **(2001)**.

[69] A.Carol, K.Laubernds, N.M.Rodriguez, R.T.K.Baker; J.Phys.Chem.B, **105**, 1115 **(2001)**.

[70] T.Maiyalagan, B.Viswanathan, U.Varadaraju; Electro.Chem.Commun, **7**, 905 (2005).

[71] W.H.Zhang, J.L.Shi, L.Z.Wang, D.S.Yan; Chem.Mater, **12**, 1408 **(2000)**.

[72] S.L.Knupp, W.Li, O.Paschos, T.M.Murray, J.Snyder, P.Haldar; Carbon, **46**, 1276 **(2008)**.

[73] T.Maiyalagan, B.Viswanathan, U.Varadaraju; Electrochemistry Communications, **7**, 905 **(2005)**.

[74] A.Kongkanand, S.Kuwabata, G.Girishkumar, P.Kamat; Langmuir, **22**, 2392 **(2006)**.

[75] X.Wang, W.Li, Z.Chen, M.Waje, Y.Yan; Journal of Power Sources, **158**, 154 **(2006)**.

[76] J.W.Long, R.M.Stroud, K.E.Swider-Lyons, D.R.Rolison; J.Phys.Chem.B, **104**, 9772 **(2000)**.

[77] Q.Lu, B.Yang, L.Zhuang, J.Lu; The Journal of Physical Chemistry B, **109**, 1715 **(2005)**.

[78] L.Jiang, G.Sun, S.Sun, J.Liu, S.Tang, H.Li, B.Zhou, Q.Xin; Electrochim Acta, **50**, 5384 **(2005)**.

[79] L.Jiang, L.Colmenares, Z.Jusys, G.Sun, R.Behm; Electrochimica Acta, **53**, 377 **(2007)**.

[80] K.W.Park, K.S.Ahn, Y.C.Nah, J.H.Choi, Y.E.Sung; The Journal of Physical Chemistry B, **107**, 4352 **(2003)**.

[81] V.Raghuveer, B.Viswanathan; J.Power Sources, **144**, 1 **(2005)**.

[82] V.Tsakova; J.Solid State Electrochem, **12**, 1421 **(2008)**.

[83] W.Napporn, H.Laborde, J.M.Leger, C.Lamy; J.Electroanal.Chem., **404**, 153 **(1996)**.

[84] M.Hepel; J.Electro.Chem.Soc., **145**, 124 **(1998)**.

[85] E.Antolini, E.Gonzalez, Appl.Phys.A:General, **365**, 1 **(2009)**.

[86] E.Antolini, E.R.Gonzalez; Applied Catalysis B: Environmental, **96**, 245 **(2010)**.

[87] S.Sharma, B.G.Pollet; J.Power Sources, **208**, 96 **(2012)**.

[88] P.Yang, Y.Wu, R.Fan; Int.J.Nano.Sci., **1**, 1 **(2002)**.

[89] Y.Wu, H.Yan, M.Huang, B.Messer, J.H.Song, P.Yang; Chemistry-A European Journal, **8**, 1260 **(2002)**.

[90] P.Yang, H.Yan, S.Mao, R.Russo, J.Johnson, R.Saykally, N.Morris, J.Pham, R.He, H.J.Choi; Adv.Funct.Mater, **12**, 323 **(2002)**.

[91] Z.L.Wang; Materials today, **7**, 26 **(2004)**.

[92] B.Wu, A.Heidelberg, J.J.Boland; Nat mater, **4**, 525 **(2005)**.

[93] A.S.Edelstein, R.C.Cammarata; Nanomaterials: Synthesis, Properties, and Applications. (Taylor & Francis), **(1998)**.

[94] H.S.Nalwa; Handbook of nanostructured materials and nanotechnology. (Academic press), **(2000)**.

[95] Y.Xia, P.Yang, Y.Sun, Y.Wu, B.Mayers, B.Gates, Y.Yin, F.Kim, H.Yan; Adv Mater, **15**, 353 **(2003)**.

[96] K.S.Shankar, A.Raychaudhuri; Mater.Sci.Eng.C, **25**, 738 **(2005)**.

[97] J.Hu, T.W.Odom, C.M.Lieber; Acc.Chem.Res., **32**, 435 **(1999)**.

[98] P.Yang; The chemistry of nanostructured materials. (World Scientific Pub Co Inc), **(2003)**

[99] C.N.R.Rao; The chemistry of nanomaterials: Synthesis, properties and applications. (Wiley-VCH), **(2006)**

[100] G.Cao; Nanostructures & nanomaterials: synthesis, properties & applications. (Imperial College Pr), **(2004)**

[101] Z.L.Wang Nanowires, Nanobelts; Materials, Properties and Devices: Volume 1: Metal and Semiconductor Nanowires. (Springer Verlag), **(2005)**

[102] Y.Wu, P.Yang; Journal of the American Chemical Society, **123**, 3165 **(2001)**.

[103] C.C.Chen, C.C.Yeh; Adv.Mater., **12**, 738 **(2000)**.

[104] M.H.Huang, Y.Wu, H.Feick, N.Tran, E.Weber, P.Yang; Adv.Mater, **13**, 113 **(2001)**.

[105] M.Yazawa, M.Koguchi, A.Muto, M.Ozawa, K.Hiruma; App.Phy.Let., **61**, 2051 **(1992)**.

[106] Y.Wu, R.Fan, P.Yang; Nano.Lett., **2**, 83 **(2002)**.

[107] Y.Choi, W.S.Kim, Y.S.Park, S.M.Lee, D.J.Bae, Y.H.Lee, G.S.Park, W.B.Choi, N.S.Lee, J.M.Kim; Adv.Mater., **12**, 746 **(2000)**.

[108] T.J.Trentler, K.M.Hickman, S.C.Goel, A.M.Viano, P.C.Gibbons, W.E.Buhro; Science, **270**, 1791 **(1995)**.

[109] J.D.Holmes, K.P.Johnston, R.C.Doty, B.A.Korgel; Science, **287**, 1471 **(2000)**.

[110] M.Gandelman, D.Milstein; Chem.Commun, 1603 **(2000)**.

[111] Y. Li,G.Meng, L.Zhang, F.Phillipp; App.Phy.Let., **76**, 2011 **(2000)**.

[112] Z.Dai, J.Gole, J.Stout, Z. Wang; J.Phys.Chem.B, **106**, 1274 **(2002)**.

[113] H.Y.Lu, S.Y.Chu, S.H.Cheng; Journal of Crystal Growth, **274**, 506 **(2005)**.

[114] H.Dang, J.Wang, S.Fan; Nanotechnology, **14**, 738 **(2003)**.

[115] R.Ryoo, C.H.Ko, M.Kruk, V.Antochshuk, M.Jaroniec; J.Phys.Chem.B, **104**, 11465 **(2000)**.

[116] Y.J.Han, J.M.Kim, G.D.Stucky; Chem.Mater., **12**, 2068 **(2000)**.

[117] M.H.Huang, A.Choudrey, P.Yang; Chem.Commun., 1063 **(2000)**.

[118] H.J.Shin, C.H.Ko, R.Ryoo; J.Mater.Chem., **11**, 260 **(2001)**.

[119] O.S.Alexeev, S.Y.Chin, M.H.Engelhard, L.Ortiz-Soto, M.D.Amiridis; J.Phys.Chem.B, **109**, 23430 **(2005)**.

[120] H.Chhina, S.Campbell, O.Kesler; J.Power Sources, **161**, 893 **(2006)**.

[121] R.Ganesan, J.S.Lee; J.Power Sources, **157**, 217 **(2006)**.

[122] Z.Tang, G.Lu; J.Power Sources, **162**, 1067 **(2006)**.

[123] L.Jiang, G.Sun, Z.Zhou, S.Sun, Q.Wang, S.Yan, H.Li, J.Tian, J.Guo, B.Zhou; J.Phys.Chem.B, **109**, 8774 **(2005)**.

[124] A.L.Santos, D.Profeti, P.Olivi Electrochim Acta, **50**, 2615 **(2005)**.

[125] T.Okanishi, T.Matsui, T.Takeguchi, R.Kikuchi, K.Eguchi; Appl.Phys.A:General, **298**, 181 **(2006)**.

[126] M.S.Saha, R.Li, X.Sun; Electrochem.Commun., **9**, 2229 **(2007)**.

[127] L.Jankovic, D.Gournis, P.N.Trikalitis, I.Arfaoui, T.Cren, P.Rudolf, M.H.Sage, T.T.M.Palstra, B.Kooi, J.De Hosson; Nano.Lett., **6**, 1131 **(2006)**.

[128] Y.Jiang, X.M.Meng, J.Liu, Z.R.Hong, C.S.Lee, S.T.Lee; Adv.Mater, **15**, 1195 **(2003)**.

[129] Grigoriants, A.Soffer, G.Salitra, D.Aurbach; J.Power Sources, **146**, 185 **(2005)**.

[130] T.Morishita, T.Hirabayashi, T.Okuni, N.Ota, M.Inagaki; J.Power Sources, **160**, 638 **(2006)**.

[131] J.Read, D.Foster, J.Wolfenstine, W.Behl; J.Power Sources, **96**, 277 **(2001)**.

[132] M.S.Saha, R.Li, M.Cai, X.Sun; J.Power Sources **185**, 1079 **(2008)**.

[133] M.S.Saha, M.N.Banis, Y.Zhang, R.Li, X.Sun, M.Cai, F.T.Wagner; J.Power Sources, **192**, 330 **(2009)**.

[134] M.S.Saha,Y.Zhang, M.Cai, X.Sun; Int.J.Hydrogen Energy, **37**, 4 6 3 3 **(2012)**.

[135] L.B.Kong, M.Lu, M.K.Li, X.Y.Guo, H.L.Li; Chinese Physics Letters, **20**, 763 **(2003)**.

[136] K.Napolskii, P.Barczuk, S.Y.Vassiliev, A.Veresov,

G.Tsirlina, P.Kulesza; Electrochim Acta, **52**, 7910 **(2007)**.
[137] J.Yuan, K.Wang, X.Xia; Adv.Funct.Mater., **15**, 803 **(2005)**.
[138] D.Wang, R.Kou, M.P.Gil, H.P.Jakobson, J.Tang, D.Yu, Y.Lu; Journal of Nanoscience and Nanotechnology, **5**, 1904 **(2005)**.
[139] E.Menke, M.Thompson, C.Xiang, L.Yang, R.Penner; Nat.Mater., **5**, 914 **(2006)**.
[140] A.Filankembo, S.Giorgio, I.Lisiecki, M.Pileni; J.Phys.Chem.B, **107**, 7492 **(2003)**.
[141] R.Krishnaswamy, H.Remita, M.Imperor-Clerc, C.Even, P.Davidson, B.Pansu; Chem.Phys.Chem., **7**, 1510 **(2006)**.
[142] Y.Song, R.M.Garcia, R.M.Dorin, H.Wang, Y.Qiu, E.N.Coker, W.A.Steen, J.E.Miller, J.A.Shelnutt; Nano.Lett., **7**, 3650 **(2007)**.
[143] Y.Song, Y.Yang, C.J.Medforth, E.Pereira, A.K.Singh, H.Xu, Y.Jiang, C.J.Brinker, F.Van Swol, J.A.Shelnutt; J.Am.Chem.Soc., **126**, 635 **(2004)**.
[144] Y.Song, R.M.Garcia, R.M.Dorin, H.Wang, Y.Qiu, J.A.Shelnutt; Angewandte Chemie, **118**, 8306 **(2006)**.
[145] H.Wang, Y.Song, C.J.Medforth, J.A.Shelnutt; J.Am.Chem.Soc., **128**, 9284 **(2006)**.
[146] Z.Q.Tian, S.P.Jiang, Z.Liu, L.Li; Electrochem.Commun, **9**, 1613 **(2007)**.
[147] S.Sun, F.Jaouen, J.P.Dodelet; Adv.Mater, **20**, 3900 **(2008)**.
[148] G.Y.Zhao, C.L.Xu, D.J.Guo, H.Li, H.L.Li; Appl.Surf.Sci., **253**, 3242 **(2007)**.
[149] W.C.Choi, S.I.Woo; J.Power Sources, **124**, 420 **(2003)**.
[150] F.Liu, J.Y.Lee, W.Zhou; Adv.Funct.Mater, **15**, 1459 **(2005)**.
[151] G.Y.Zhao, C.L.Xu, D.J.Guo, H.Li, H.L.Li; J.Power Sources, **162**, 492 **(2006)**.
[152] G.Y.Zhao, C.L.Xu, H.L.Li; Mater.Lett, **62**, 1663 **(2008)**.
[153] Z.Liang, T.Zhao; J.Phys.Chem.C, **111**, 8128 **(2007)**.
[154] E.P.Lee, Z.Peng, D.M.Cate, H.Yang, C.T.Campbell, Y.Xia; J.Am.Chem.Soc., **129**, 10634 **(2007)**.
[155] S.Sun, D.Yang, D.Villers, G.Zhang, E.Sacher, J.P.Dodelet; Adv.Mater, **20**, 571 **(2008)**.
[156] L.Wang, S.Guo, J.Zhai, S.Dong; J.Phys.Chem.C, **112**, 13372 **(2008)**.
[157] S.Du; J.Power Sources, **195**, 289 **(2010)**.
[158] S.M.Choi, J.H.Kim, J.Y.Jung, E.Y.Yoon, W.B.Kim; Electrochim.Acta, **53**, 5804 **(2008)**.
[159] S.Du, B.Millington, B.G.Pollet; Int.J.Hydrogen Energy, **36**, 4386 **(2011)**.
[160] W.P.Zhou, M.Li, C.Koenigsmann, C.Ma, S.S.Wong, R.R.Adzic; Electrochim.Acta, **56**, 9824 **(2011)**.
[161] E.Formo, E.Lee, D.Campbell, Y.Xia; Nano Lett, **8**, 668 **(2008)**.
[162] Y.S.Kim, S.H.Nam, H.S.Shim, H.J.Ahn, M.Anand, W.B.Kim; Electrochem.Commun, **10**, 1016 **(2008)**.
[163] H.J.Kim, Y.S.Kim, M.H.Seo, S.M.Choi, W.B.Kim; Electrochem.Commun., **11**, 446 **(2009)**.
[164] C.Xu, H.Wang, P.K.Shen, S.P.Jiang; Adv.Mater, **19**, 4256 **(2007)**.
[165] Y.S.Kim, H.J.Kim, W.B.Kim; Electrochem.Commun., **11**, 1026 **(2009)**.
[166] G.R.Patzke, F.Krumeich, R.Nesper; Angewandte Chemie International Edition, **41**, 2446 **(2002)**.
[167] T.Maiyalagan, B.Viswanathan; J.Power Sources, **175**, 789 **(2008)**.
[168] J.Rajeswari, B.Viswanathan, T.K.Varadarajan; Materials Chemistry and Physics, **106**, 168 **(2007)**.
[169] D.V.Bavykin, J.M.Friedrich, F.C.Walsh; Adv.Mater., **18**, 2807 **(2006)**.
[170] J.Marugan, D.Hufschmidt, M.J.Lopez-Munoz, V.Selzer, D.Bahnemann; Appl.Catal.B :Environmental, **62**, 201 **(2006)**.
[171] A.Yamakata, T.Ishibashi, H.Onishi; J.Phys.Chem.B, **106**, 9122 **(2002)**.
[172] K.Drew, G.Girishkumar, K.Vinodgopal, P.V.Kamat; J.Phys.Chem.B, **109**, 11851 **(2005)**.
[173] H.Song, X.Qiu, F.Li, W.Zhu, L.Chen; Electrochem.Commun., **9**, 1416 **(2007)**.
[174] H.Song, X.Qiu, X.Li, F.Li, W.Zhu, L.Chen; J.Power Sources, **170**, 50 **(2007)**.
[175] S.Berger, A.Ghicov, Y.C.Nah, P.Schmuki; Langmuir, **25**, 4841 **(2009)**.
[176] W.Chanmanee, A.Watcharenwong, C.R.Chenthamarakshan, P.Kajitvichyanukul, N.R.de Tacconi, K.Rajeshwar; J.Am.Chem.Soc., **130**, 965 **(2008)**.
[177] T.S.Kang, A.P.Smith, B.E.Taylor, M.F.Durstock; Nano.Lett, **9**, 601 **(2009)**.
[178] D.Vuong, D.Tram, P.Pho, N.Chien; Physics and Engineering of New Materials 95 **(2009)**.
[179] M.Wang, D.Guo, H.Li; Journal of Solid State

Chemistry, **178**, 1996 **(2005)**.

[180] J.Macak, P.Barczuk, H.Tsuchiya, M.Nowakowska, A.Ghicov, M.Chojak, S.Bauer, S.Virtanen, P.Kulesza, P.Schmuki; Electrochemistry.Communications., **7**, 1417 **(2005)**.

[181] S.H.Kang, T.Y.Jeon, H.S.Kim, Y.E.Sung, W.H.Smyrl; J.Electrochem.Soc., **155**, B1058 **(2008)**.

[182] T.Kasuga, M.Hiramatsu, A.Hoson, T.Sekino, K.Niihara; Langmuir, **14**, 3160 **(1998)**.

[183] Z.Chen, M.Waje, W.Li, Y.Yan; Angewandte Chemie International Edition, **46**, 4060 **(2007)**.

[184] J.D.Stenger-Smith; Progress in Polymer Science, **23**, 57 **(1998)**.

[185] Y.S.Negi, P.Adhyapak; Journal of Macromolecular Science, Part C: Polymer Reviews, **42**, 35 **(2002)**.

[186] H.S.O.Chan, S.C.Ng; Progress in Polymer Science, **23**, 1167 **(1998)**.

[187] A.Rudge, I.Raistrick, S.Gottesfeld, J.P.Ferraris; Electrochim.Acta, **39**, 273 **(1994)**.

[188] K.S.Ryu, K.M.Kim, N.G.Park, Y.J.Park, S.H.Chang; J.Power Sources, **103**, 305 **(2002)**.

[189] D.Walton; Mater.Des., **11**, 142 **(1990)**.

[190] L.Dai; Intelligent macromolecules for smart devices: from materials synthesis to device applications. (Springer Verlag), **(2004)**

[191] L.Pan, L.Pu, Y.Shi, S.Song, Z.Xu, R.Zhang, Y.Zheng; Adv.Mater **19**, 461 **(2007)**.

[192] J.Huang; Pure.Appl.Chem., **78**, 15 **(2006)**.

[193] S.Xing, H.Zheng, G.Zhao; Synth.Met., **158**, 59 **(2008)**.

[194] X.Yu,Y.Li, K.Kalantar-zadeh Sens Actuators B : Chemical, **136**, 1 **(2009)**.

[195] X.Bai, X.Li, N.Li, Y.Zuo, L.Wang, J.Li, S.Qiu; Mater.Sci.Eng.C, **27**, 695 **(2007)**.

[196] C. Debiemme-Chouvy Electrochem Commun **11**, 298 **(2009)**.

[197] Y.Hu, A.To, M.Yun; Nanotechnology, **20**, 285605 **(2009)**.

[198] Z.Niu, J.Liu, L.A.Lee, M.A.Bruckman, D.Zhao, G.Koley, Q.Wang; Nano.Lett., **7**, 3729 **(2007)**.

[199] S.Park, M.Cho, J.Nam, I.Kim, H.Choi, J.Koo, Y.Lee; Sens Actuators B : Chemical, **135**, 592 **(2009)**.

[200] L.S.Van Dyke, C.R.Martin; Langmuir, **6**, 1118 **(1990)**.

[201] Z.Cai, C.R.Martin; J.Am.Chem.Soc., **111**, 4138 **(1989)**.

[202] B.Rajesh, K.R.Thampi, J.Bonard, H.Mathieu, N.Xanthopoulos, B.Viswanathan; Electrochem Solid-State Lett., **7**, A404 **(2004)**.

[203] B.Rajesh, K.R.Thampi, J.M.Bonard, A.McEvoy, N.Xanthopoulos, H.Mathieu, B.Viswanathan; J.Power Sources, **133**, 155 **(2004)**.

[204] Y.Huang, C.Lin, C.Chang, M.Ho; Electrochim Acta, **56**, 5679 **(2011)**.

[205] M.Zhiani, H.Gharibi, K.Kakaei; J.Power Sources, **210**, 42 **(2012)**.

[206] E.Antolini; Appl.Catal, B :Environmental, **100**, 413 **(2010)**.

[207] J.Shi, D.Guo, Z.Wang, H.Li; J.Solid State Electrochem, **9**, 634 **(2005)**.

[208] J.Shi, Z.Wang, H.Li; J.Mater.Sci., **42**, 539 **(2007)**.

[209] G.Wu, L.Li, J.H.Li, B.Q.Xu; J.Power Sources, **155**, 118 **(2006)**.

[210] Z.Wang, Z.Z.Zhu, J.Shi, H.L.Li; Appl.Surf.Sci., **253**, 8811 **(2007)**.

[211] Z.Z.Zhu, Z.Wang, H.L.Li; Appl.Surf.Sci., **254**, 2934 **(2008)**.

[212] P.Santhosh, A.Gopalan, K.P.Lee; J.Catal., **238**, 177 **(2006)**.

[213] V.Selvaraj, M.Alagar; Electrochem.Commun, **9**, 1145 **(2007)**.

[214] B.Qu, Y.T.Xu, S.Lin, Y.F.Zheng, L.Z.Dai; Synth.Met., **160**, 732 **(2010)**.

[215] H.B.Bae, J.H.Ryu, B.S.Byun, S.H.Jung, S.H.Choi; Current Applied Physics, **10**, S44 **(2010)**.

[216] C.Jiang, H.Chen, C.Yu, S.Zhang, B.Liu; J.Kong Electrochim Acta, **54**, 1134 **(2009)**.

[217] Z.C.Wang, Z.M.Ma, H.L.Li; Appl.Surf.Sci., **254**, 6521 **(2008)**.

[218] H.S.Oh, K.Kim, H.Kim; Int.J.Hydrogen Energy, **36**, 1 1 5 6 4 **(2011)**.

[219] A.Bauer, R.Hui, A.Ignaszak, J.Zhang, D.J.Jones; J.Power Sources, **210**, 15 **(2012)**.

[220] F.Hu, G.Cui, Z.Wei, P.K.Shen; Electrochem.Commun, **10**, 1303 **(2008)**.

[221] C.Du, M.Chen, X.Cao, G.Yin, P.Shi; Electrochem.Commun; **11**, 496 **(2009)**.

[222] N.Jha, R.I.Jafri, N.Rajalakshmi, S.Ramaprabhu; Int.J.Hydrogen Energy, **36**, 7 2 8 4 **(2011)**.

[223] M.S.Saha, R.Li, M.Cai, X.Sun; Electrochem Solid-State Lett., **10**, B130 **(2007)**.

[224] C.L.Ku; MS theses, **(2007)**.